Electronic Supplementary Material (ESI) for Chemical Communications.
This journal is © The Royal Society of Chemistry 2024

Electronic Supplementary Information for

Crystallographic and spectroscopic studies on persistent triarylpropargyl cations

Takuya Shimajiri,[*a,b] Taiga Tsue,[a] Shumpei Koakutsu,[a] Yusuke Ishigaki,[a] Takanori Suzuki[*a]

[a]*Department of Chemistry, Faculty of Science, Hokkaido University, Sapporo 060-0810, Japan.*
[b]*Creative Research Institution, Hokkaido University, Sapporo, Hokkaido 001-0021, Japan*
[c]*Present address: Department of Applied Chemistry, Graduate School of Engineering, Kyushu University, 819-0395, Japan*

E-mail: t.shimajiri@sci.hokudai.ac.jp, tak@sci.hokudai.ac.jp

Table of contents

1. General

All reactions were carried out under an argon atmosphere. All commercially available compounds were used without further purification. Dry acetonitrile was obtained by distillation from CaH_2 and P_2O_5 prior to use. Column chromatography was performed on silica gel 60N (KANTO KAGAKU, spherical neutral) of particle size 40–50 μm or Wakogel® 60N (neutral) of particle size 38-100 μm. ^1H and ^{13}C NMR spectra were recorded on a BRUKER Ascend™ 400 (^1H/400 MHz and ^{13}C/100 MHz) spectrometer. IR spectra were measured on a Shimadzu IRAffinity-1S spectrophotometer using the attenuated total reflection (ATR) mode. Mass spectra were recorded on a JEOL JMS-T100GCV spectrometer in FD mode (GC-MS&NMR Laboratory, Research Faculty of Agriculture, Hokkaido University). Melting points were measured on a Stanford Research Systems MPA100 Optimelt and are uncorrected. UV-Vis spectra in solution state were recorded on a JASCO V-770 spectrophotometer. UV-Vis spectra in a solid state were recorded on a JASCO MSV 5200 spectrophotometer (Transmittance Mode). DFT calculations were performed with the Gaussian 16W program package [1]. All calculations were performed at B3LYP-D3/6-31G** level of theory.

2. Experimental Section

2.1 Synthetic procedures

Scheme S1. Synthetic route for propargyl cations $\mathbf{1}^{+}X^{-}$, $\mathbf{2}^{+}X^{-}$

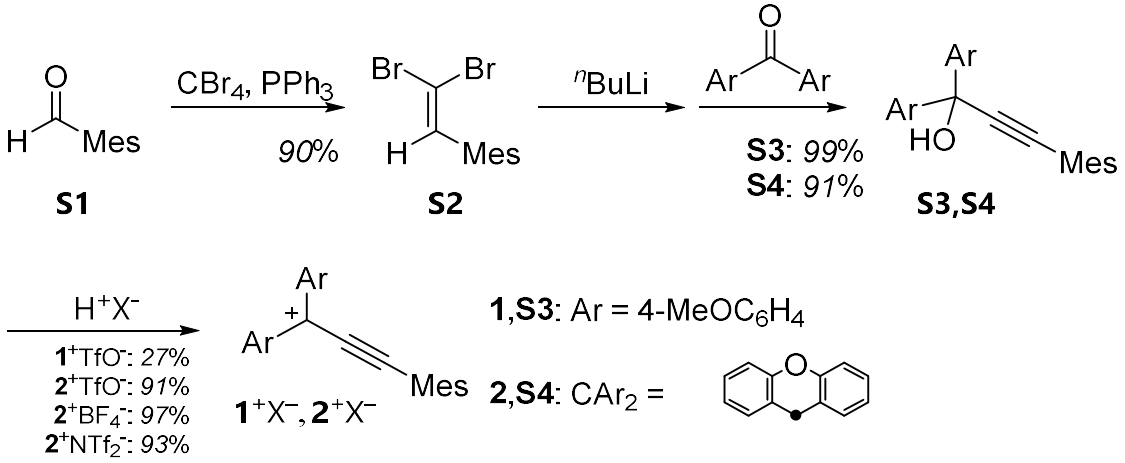

3-mesityl-1,1-bis(4-methoxyphenyl)prop-2-yn-1-ol **S3**

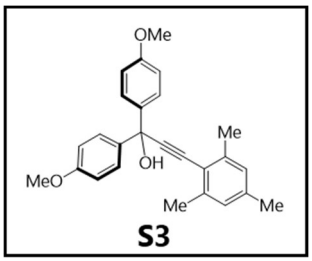

To a solution of **S2** (3.04 g, 10.0 mmol) prepared from **S1** according to the reported method[2] in dry THF (50 mL) was added ^{n}BuLi (1.52 M in hexane, 14.0 mL, 21.3 mmol) dropwise over 5 min at -78 °C. After stirring at -78 °C for 30 min, 4,4'-dimethoxybenzophenone (2.42 g, 10.0 mmol) was added to the reaction mixture at -78 °C. The mixture was warmed to 26 °C and stirred at 26 °C for 2 h. Then, the mixture was diluted with water (20 mL). The whole mixture was extracted with EtOAc (30 mL) three times. The combined organic layers were washed with water and brine, and dried over anhydrous $MgSO_4$. After filtration, the solvent was concentrated under reduced pressure. The crude product was purified by column chromatography on silica gel (EtOAc:hexane = 1:19, Rf = 0.38) to give **S3** (3.84 g, 9.93 mmol, 99% yield) as a viscous golden yellow oil.

S3; ^{1}H NMR (400 MHz, $CDCl_3$): δ/ppm 7.59 (4H, d, *J*= 8.8 Hz), 6.86 (2H, s), 6.86 (4H, d, *J*= 8.8 Hz), 3.80 (6H, s), 2.76 (1H, s), 2.39 (6H, s), 2.28 (3H, s); ^{13}C NMR (100 MHz, $CDCl_3$): δ/ppm 159.02, 140.45, 138.04, 137.91, 127.63, 127.46, 119.30, 113.49, 99.87, 85.02, 74.64, 55.29, 21.29, 21.11; IR (ATR): ν/cm^{-1} 3454, 2951, 2943, 2914, 2835, 2365, 2217, 1608, 1584, 1506, 1462, 1441, 1416, 1374, 1300, 1244, 1171, 1115, 1033, 988, 935, 901, 854, 828, 783, 750, 729, 636, 619, 587, 548; LR-MS (FD) m/z (%): 388.24 (5), 387.24 (30), 386.23 (M^{+}, bp); HR-MS (FD) Calcd. for $C_{26}H_{26}O_3$: 386.18819; Found: 386.18920.

9-(mesitylethynyl)-9*H*-xanthen-9-ol **S4**

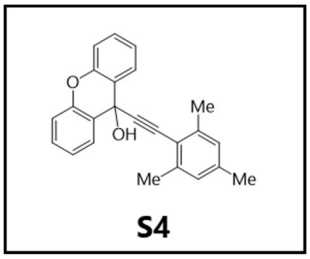

S4

To a solution of **S2** (10.0 g, 32.9 mmol) prepared from **S1** according to the reported method[2] in dry THF (150 mL) was added ^{n}BuLi (1.51 M in hexane, 43.5 mL, 65.8 mmol) dropwise over 15 min at -78 °C. After stirring at -78 °C for 30 min, xanthone (5.87 g, 29.9 mmol) was added to the reaction mixture at -78 °C. The mixture was warmed to 26 °C and stirred at 26 °C for 29 h. Then, the mixture was diluted with water (50 mL). The whole mixture was extracted with EtOAc (30 mL) three times. The combined organic layers were washed with water and brine and dried over anhydrous $MgSO_4$. After filtration, the solvent was concentrated under reduced pressure. The crude product was purified by washing with hexane (100 mL) to give **S4** (9.21 g, 27.1 mmol, 91% yield) as a white solid.

S4; Mp: 117.3-117.9°C; ^{1}H NMR (400 MHz, $CDCl_3$): δ/ppm 8.08 (2H, dd, *J*= 0.8 Hz, 8.0 Hz), 7.40 (2H, ddd, *J*= 0.8 Hz, 7.8 Hz, 7.9 Hz), 7.20-7.26 (4H, m), 6.86 (2H, s), 2.73 (1H, s), 2.41 (6H, s), 2.28 (3H, s); ^{13}C NMR (100 MHz, $CDCl_3$): δ/ppm 149.63, 140.54, 138.30, 129.93, 128.73, 127.67, 124.20, 123.59, 119.00, 116.85, 98.25, 85.78, 64.98, 21.32, 21.09; IR (ATR): ν/cm^{-1} 3486, 3048, 2914, 2854, 2729, 2228, 1952, 1910, 1768, 1742, 1622, 1605, 1576, 1490, 1480, 1458, 1447, 1378, 1366, 1319, 1293, 1236, 1205, 1151, 1127, 1101, 1034, 1016, 965, 939, 926, 906, 873, 866, 826, 763, 753, 744, 729, 722, 675, 631, 592, 576, 542, 501; LR-MS (FD) m/z (%): 342.15 (4), 341.15 (26), 340.14 (M^+, bp); HR-MS (FD) Calcd. for $C_{24}H_{20}O_2$: 340.14633; Found: 340.14513.

3-mesityl-1,1-bis(4-methoxyphenyl) prop-2-yn-1-ylium triflate **1**$^{+}$TfO^{-}

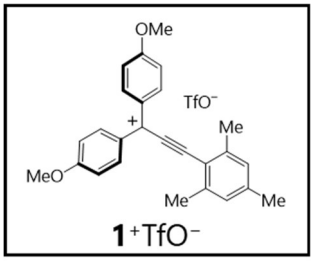

1^{+}TfO^{-}

To a solution of **S3** (200 mg, 517 μmol) in dry CH_2Cl_2 (1.0 mL) was added TfOH (140 μL, 1.55 mmol) at -40 °C, and the mixture was stirred at -40 °C for 20 min. The addition of dry diethyl ether led to precipitation of the cation salt at -40°C. The precipitates were collected, washed with dry diethyl ether (20 mL) three times, and dried in vacuo to give **1**$^{+}$TfO^{-} (71.8 mg, 138 μmol, 27% yield) as a red solid.

1^{+}TfO^{-}; Mp: 96.9-114.5 °C (decomp.); ^{1}H NMR (400 MHz, $CDCl_3$): δ/ppm 8.16 (4H, d, *J*= 9.2 Hz), 7.35 (4H, d, *J*= 9.2 Hz), 7.09 (2H, s), 4.15 (6H, s), 2.59 (6H, s), 2.42 (3H, s); ^{13}C NMR (100 MHz, $CDCl_3$ with 2.6% w/v TFAA): δ/ppm 171.67, 171.64, 147.95, 146.36, 141.14, 138.04, 132.26, 129.46, 117.97, 117.49, 106.90, 57.30, 22.13, 21.44; IR (ATR): ν/cm^{-1} 3097, 3007, 2955, 2850, 2735, 2642, 2605, 2321, 2130, 2115, 1594, 1577, 1513, 1464, 1451, 1440, 1378, 1352, 1318, 1276, 1225, 1179, 1154, 1131, 1063, 1029, 914, 827, 807, 785, 755, 722, 664, 635, 610, 602, 579, 553, 547, 512; LR-MS (FD) m/z (%): 386.17 (13), 370.18 (29), 369.17 (M^+, bp); HR-MS (FD) Calcd. for $C_{26}H_{25}O_2$: 369.18511; Found: 369.18545.

9-(mesitylethynyl)-9*H*-xanthen-9-ylium triflate **2**$^{+}$TfO^{-}

To a solution of **S4** (3.00 g, 8.81 mmol) in dry CH_2Cl_2 (15.0 mL) was added TfOH (857 µL, 9.69 mmol) at 0 °C, and the mixture was stirred at 0 °C for 5 min. The addition of dry diethyl ether led to precipitation of the cation salt at 0°C. The precipitates were collected, washed with dry diethyl ether (100 mL) three times, and dried in vacuo to give **2**$^{+}$TfO^{-} (4.03 g, 8.53 mmol, 91% yield) as a red solid.

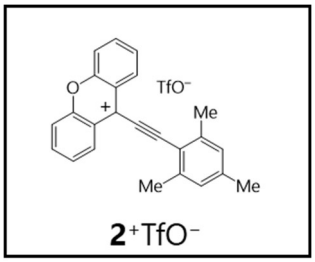

2^{+}TfO^{-}; Mp: 145.9-146.7 °C (decomp.); ^{1}H NMR (400 MHz, $CDCl_3$): δ/ppm 8.82 (2H, dd, *J*= 1.2 Hz, 8.4 Hz), 8.54 (2H, ddd, *J*= 1.6 Hz, 7.0 Hz, 8.7 Hz), 8.27 (2H, dd, *J*= 1.2 Hz, 8.8 Hz), 8.09 (2H, ddd, *J*= 1.2 Hz, 7.2 Hz, 8.3 Hz), 7.22 (2H, s), 2.82 (6H, s), 2.45 (3H, s); ^{13}C NMR (100 MHz, $CDCl_3$): δ/ppm 157.96, 154.83, 148.13, 146.49, 144.02, 132.15, 130.76, 130.05, 129.88, 124.74, 120.39, 97.75, 21.83; IR (ATR): ν/cm^{-1} 3087, 2982, 2313, 2229, 2131, 1616, 1594, 1577, 1544, 1493, 1473, 1436, 1392, 1369, 1291, 1268, 1235, 1223, 1173, 1136, 1065, 1031, 1010, 954, 913, 881, 868, 835, 789, 773, 749, 727, 668, 635, 627, 617; LR-MS (FD) m/z (%): 324.15 (27), 323.15 (M^{+}, bp); HR-MS (FD) Calcd. for $C_{24}H_{19}O$: 323.14359; Found: 323.14504.

9-(mesitylethynyl)-9*H*-xanthen-9-ylium tetrafluoroborate **2**$^{+}$$BF_4^{-}$

To a solution of **S4** (300 mg, 881 µmol) in dry CH_2Cl_2 (3.00 mL) was added HBF_4• Et_2O (157 mg, 969 µmol) at 0 °C, and the mixture was stirred at 0 °C for 5 min. The addition of dry diethyl ether led to precipitation of the cation salt at 0°C. The precipitates were collected, washed with dry diethyl ether (30 mL) three times, and dried in vacuo to give **2**$^{+}$$BF_4^{-}$ (352 mg, 858 µmol, 97% yield) as a red solid.

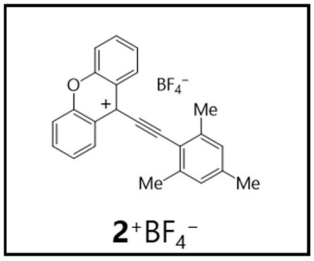

2^{+}BF_4^{-}; Mp: 231.2-232.0 °C (decomp.); ^{1}H NMR (400 MHz, $CDCl_3$): δ/ppm 8.83 (2H, dd, *J*= 1.2 Hz, 8.3 Hz), 8.53 (2H, ddd, *J*= 1.6 Hz, 7.8 Hz, 8.0 Hz), 8.30 (2H, dd, *J*= 0.8 Hz, 8.8 Hz), 8.10 (2H, ddd, *J*=1.2Hz, 7.2 Hz, 8.4 Hz), 7.20 (2H, s), 2.81 (6H, s), 2.44 (3H, s); ^{13}C NMR (100 MHz, CD_3CN with 4.6% w/v TFAA): δ/ppm 157.92, 154.70, 148.20, 146.52, 144.07, 132.14, 130.72, 130.10, 129.89, 124.69, 120.42, 21.87; IR (ATR): ν/cm^{-1} 3096, 2360, 2332, 2226, 2138, 1618, 1594, 1577, 1545, 1494, 1474, 1436, 1392, 1369, 1294, 1244, 1236, 1210, 1175, 1165, 1122, 1092, 1050, 1034, 1020, 1011, 956, 881, 835, 788, 747, 727, 668, 643, 628, 617; LR-MS (FD) m/z (%): 324.11 (28), 323.11 (M^{+}, bp); HR-MS (FD) Calcd. for $C_{24}H_{19}O$: 323.14359; Found: 323.14340.

9-(mesitylethynyl)-9*H*-xanthen-9-ylium bis(trifluoromethanesulfonyl)imide **2**$^{+}$NTf$_2^{-}$

To a solution of **S4** (300 mg, 881 μmol) in dry CH_2Cl_2 (3.00 mL) was added $HNTf_2$ (273 mg, 969 μmol) at 0 °C, and the mixture was stirred at 0 °C for 5 min. The addition of dry diethyl ether led to precipitation of the cation salt at 0°C. The precipitates were collected, washed with dry diethyl ether (50 mL) three times, and dried in vacuo to give **2**$^{+}$NTf$_2^{-}$ (493 mg, 818 μmol, 93% yield) as a red solid.

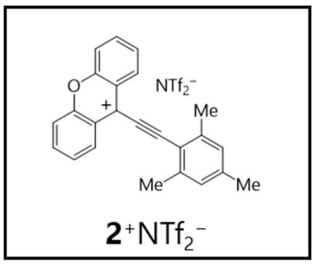

2^{+}NTf$_2^{-}$

2^{+}NTf$_2^{-}$; Mp: 193.6-195.8 °C (decomp.); ^{1}H NMR (400 MHz, $CDCl_3$): δ/ppm 8.82 (2H, br-d, *J*= 8.0 Hz), 8.53 (2H, br-t, *J*= 7.2 Hz), 8.27 (2H, br-d, *J*= 8.8 Hz), 8.09 (2H, ddd, *J*= 0.8 Hz, 7.2 Hz), 7.21 (2H, s), 2.82 (6H, s), 2.45 (3H, s); ^{13}C NMR (100 MHz, $CDCl_3$): δ/ppm 157.86, 154.59, 148.17, 146.48, 144.04, 132.09, 130.67, 130.07, 129.86, 124.63, 120.39, 97.81, 21.06; IR (ATR): ν/cm^{-1} 3082, 2315, 2150, 1615, 1594, 1578, 1542, 1494, 1472, 1436, 1395, 1370, 1350, 1333, 1294, 1240, 1200, 1175, 1160, 1136, 1053, 1038, 935, 895, 880, 861, 834, 792, 757, 743, 725, 667, 644, 610; LR-MS (FD) m/z (%): 324.14 (27), 323.14 (M^{+}, bp); HR-MS (FD) Calcd. for $C_{24}H_{19}O$: 323.14359; Found: 323.14344.

2.2 NMR spectra of new compounds

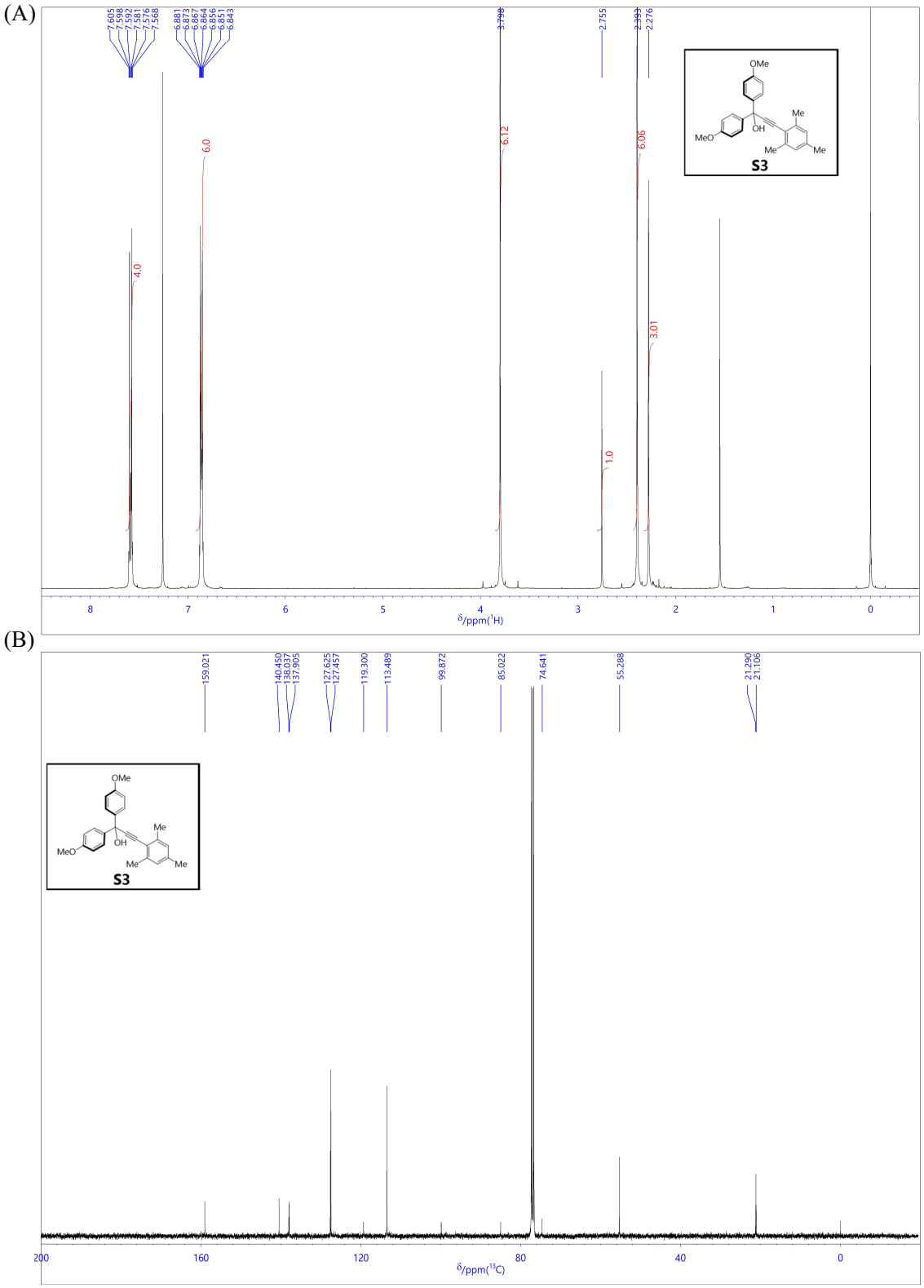

Figure S1. (A) ^{1}H NMR and (B) ^{13}C NMR spectra of **S3** in $CDCl_3$.

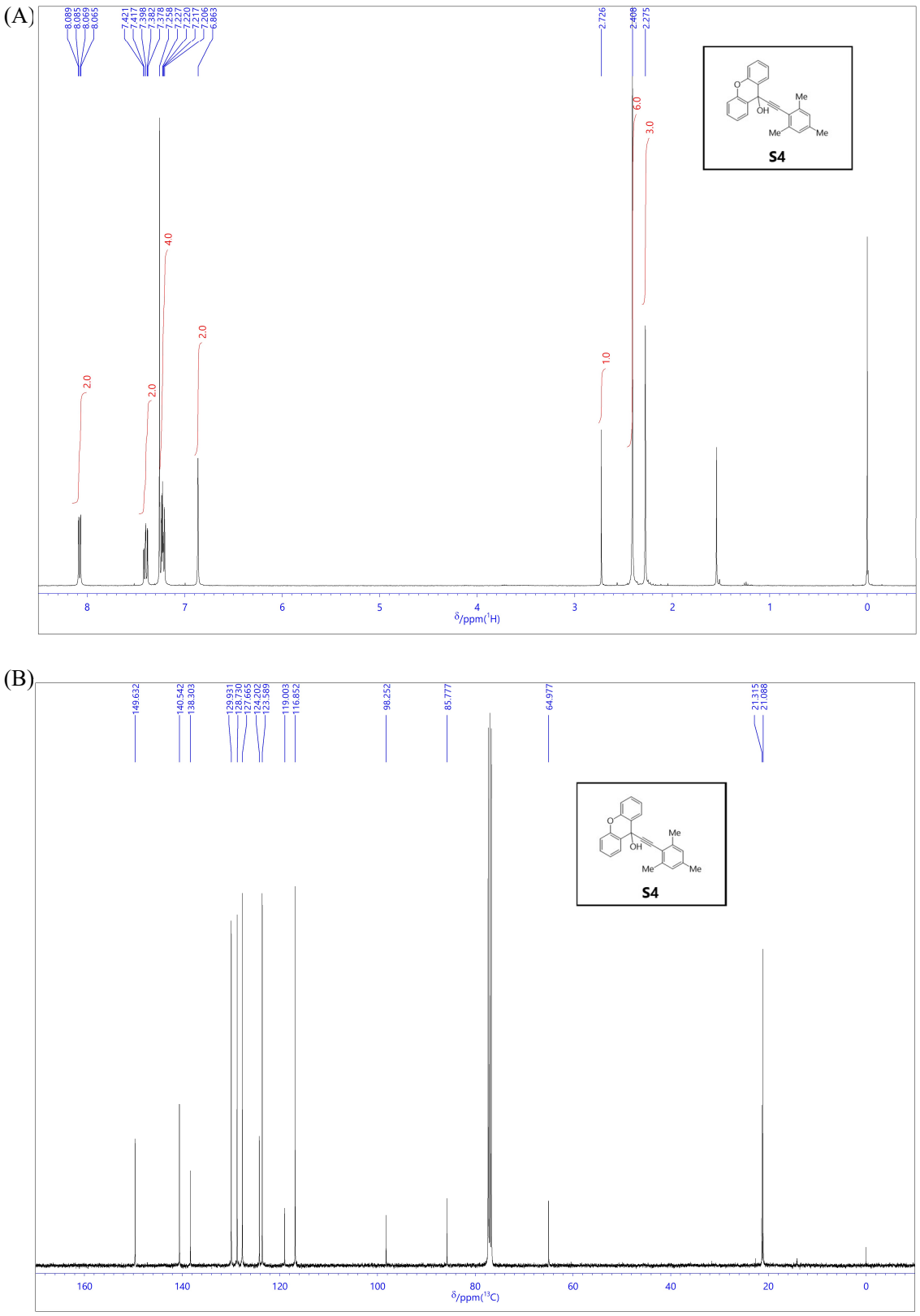

Figure S2. (A) ^{1}H NMR and (B) ^{13}C NMR spectra of **S4** in $CDCl_3$.

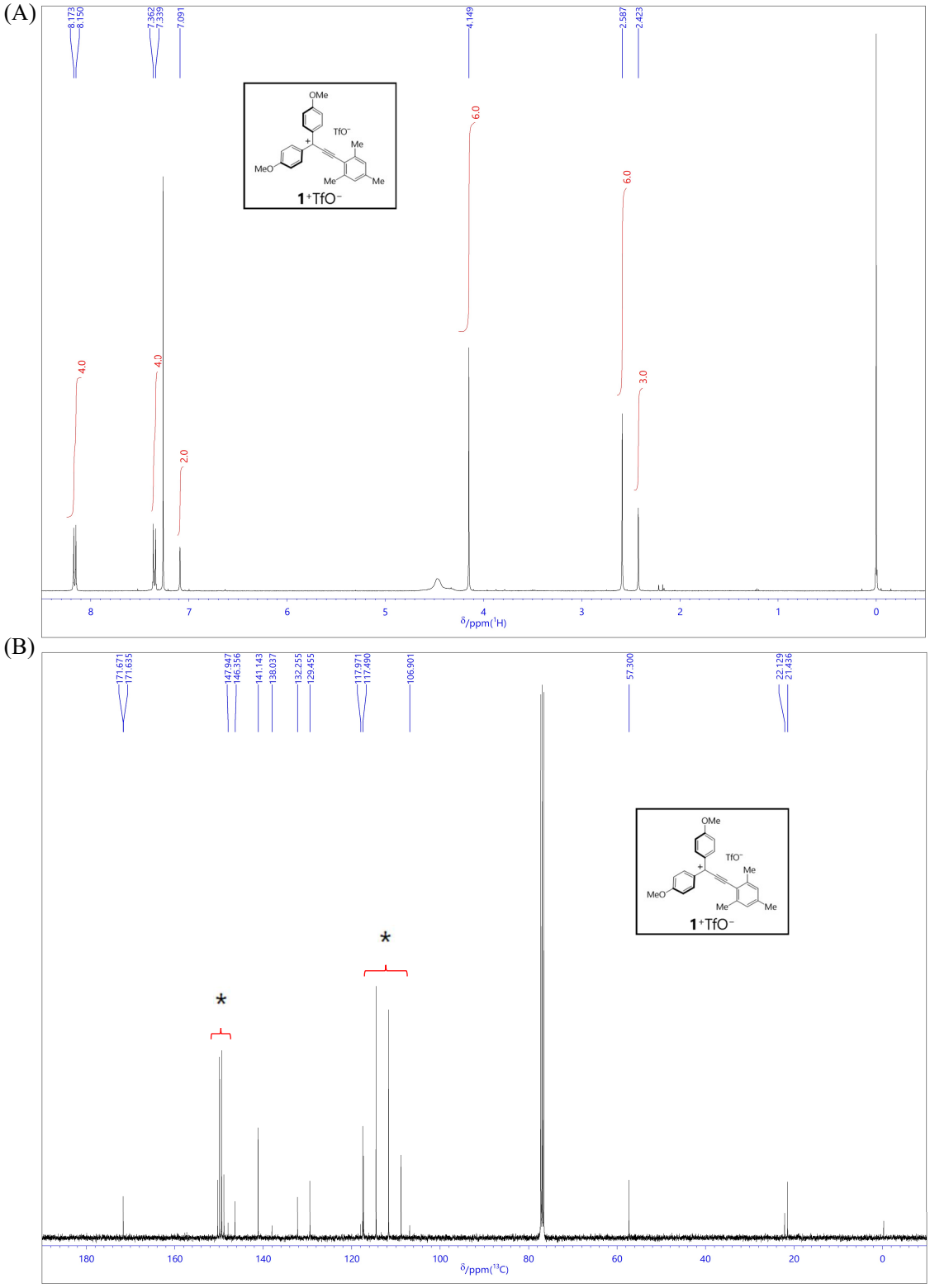

Figure S3. (A) ^{1}H NMR and (B) ^{13}C NMR spectra of $1^{+}TfO^{-}$ in $CDCl_3$.

In (B), TFAA was added to $\mathbf{1}^{+}TfO^{-}$ for stabilization.

* shows TFAA peaks.

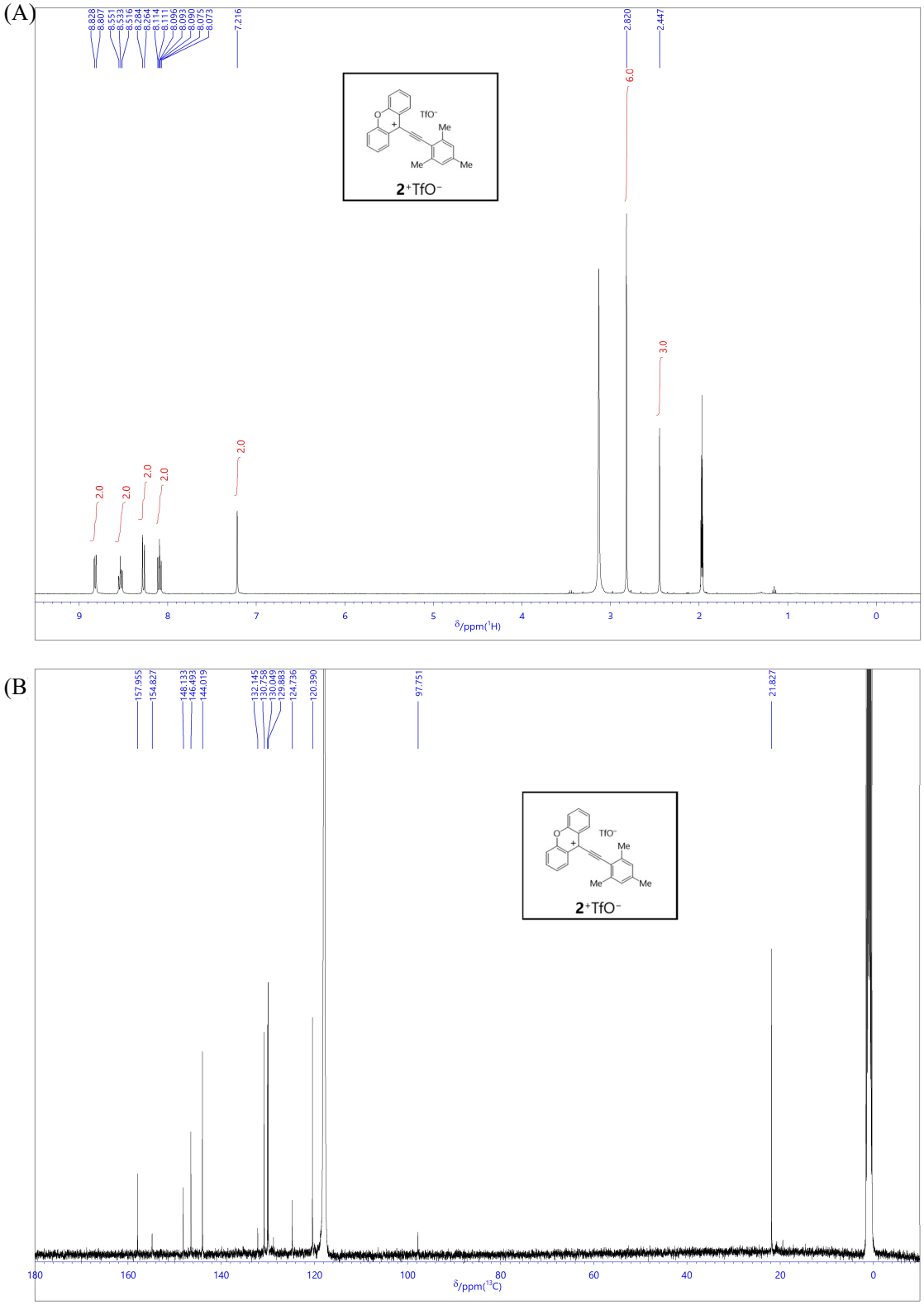

Figure S4. (A) ^{1}H NMR and (B) ^{13}C NMR spectra of **2**$^{+}$TfO^{-} in CD_3CN.

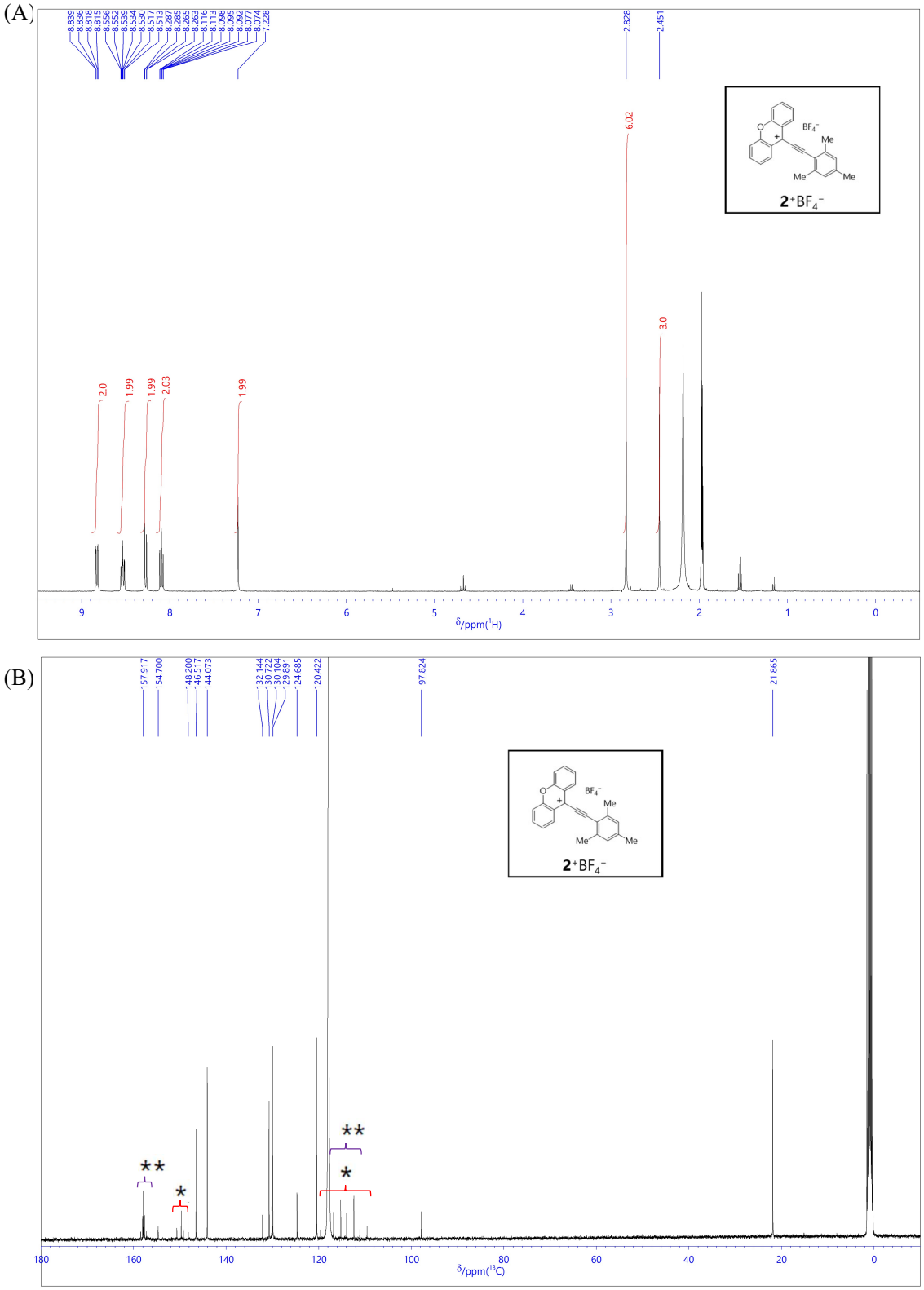

Figure S5. (A) ^{1}H NMR and (B) ^{13}C NMR spectra of $\mathbf{2}^{+}BF_4^{-}$ in CD_3CN.

In (B), TFAA was added to $\mathbf{2}^{+}BF_4^{-}$ for stabilization.

* shows TFAA peaks. ** shows TFA peaks.

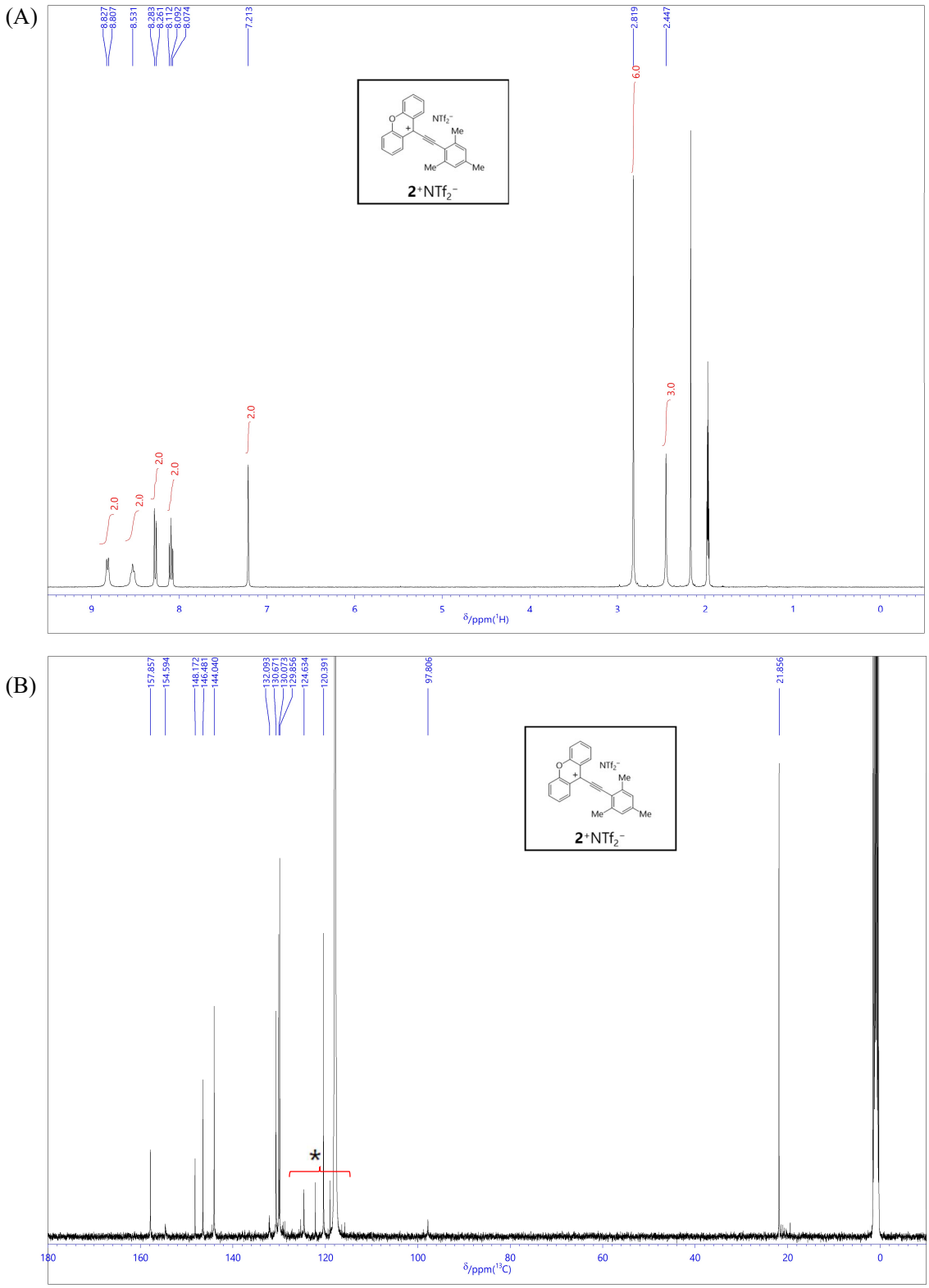

Figure S6. (A) ^{1}H NMR and (B) ^{13}C NMR spectra of $\mathbf{2}^{+}NTf_2^{-}$ in CD_3CN.

* shows NTf_2^{-} peak.

2.3 FD-MS spectra of new compounds

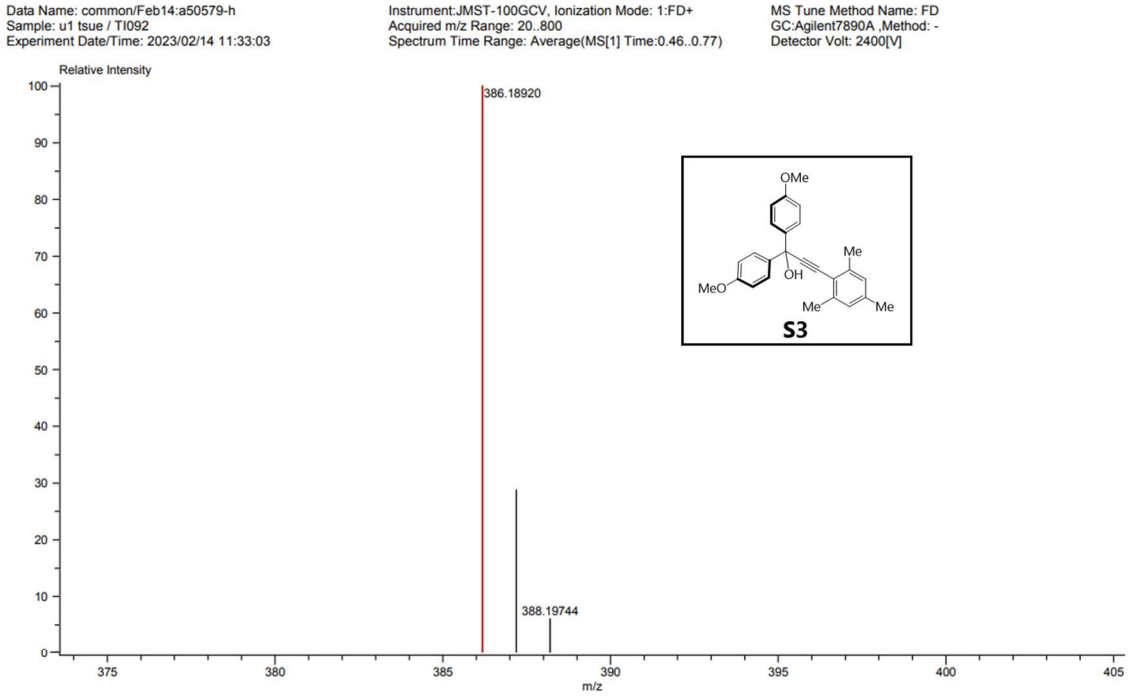

Data:a50579-h
Sample Name:u1 tsue / TI092
Description:
Ionization Mode:FD+
History:Determine m/z[Peak Detect[Centroid,20,Area];Correct Base[];Smooth[5]];Smooth[5];Average(MS[1] 0.46..0.77)

Acquired:2023/02/14 11:33:03
Operator:Administrator
Mass Calibration data:800K
Created:2023/02/14 16:32:02
Created by:Administrator

Charge number:1
Element:^{12}C:0 .. 100, ^{1}H:0 .. 200, ^{16}O:0 .. 10

Tolerance:5.00(mmu)

Unsaturation Number:-1.5 .. 20.0 (Fraction:Both)

Mass	Calc. Mass	Mass Difference (mmu)	Mass Difference (ppm)	Possible Formula	Unsaturation Number
386.18920	386.18819	1.01	2.62	$^{12}C_{26}{}^{1}H_{26}{}^{16}O_3$	14.0
	386.19407	-4.86	-12.59	$^{12}C_{19}{}^{1}H_{30}{}^{16}O_8$	5.0

Figure S7. A HR-MS spectrum of **S3**.

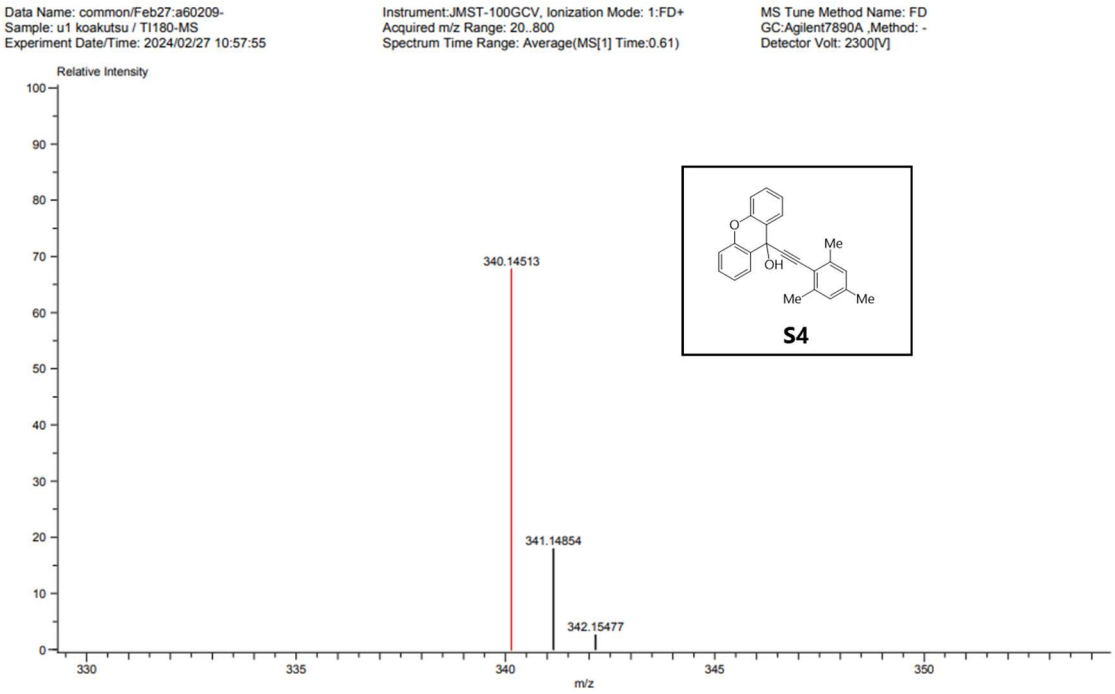

Data:a60209-
Sample Name:u1 koakutsu / TI180-MS
Description:
Ionization Mode:FD+
History:Determine m/z[Peak Detect[Centroid,10,Area];Correct Base[];Smooth[5]];Smooth[5];Average(MS[1] 0.61)

Acquired:2024/02/27 10:57:55
Operator:Administrator
Mass Calibration data:800P6
Created:2024/02/27 11:01:51
Created by:Administrator

Charge number:1
Tolerance:5.00(mmu)
Unsaturation Number:-1.5 .. 20.0 (Fraction:Both)
Element: ^{12}C:0 .. 100, ^{1}H:0 .. 200, ^{16}O:0 .. 10

Mass	Calc. Mass	Mass Difference (mmu)	Mass Difference (ppm)	Possible Formula	Unsaturation Number
340.14513	340.14633	-1.20	-3.52	$^{12}C_{24}{}^{1}H_{20}{}^{16}O_2$	15.0

Figure S8. A HR-MS spectrum of **S4**.

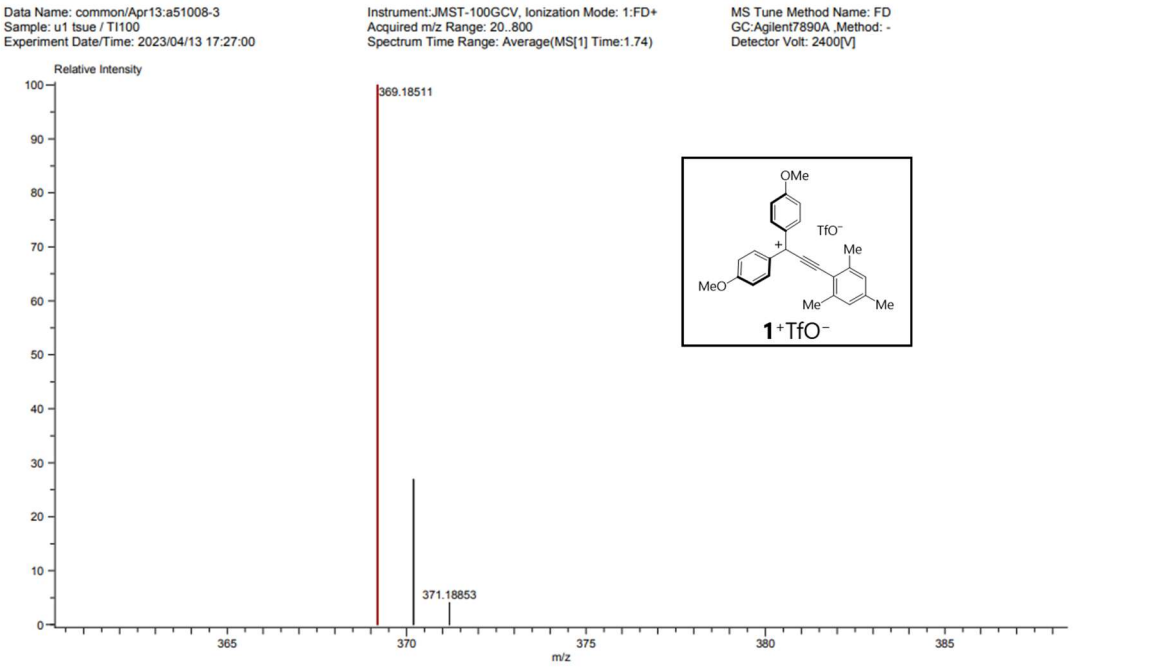

Mass	Calc. Mass	Mass Difference (mmu)	Mass Difference (ppm)	Possible Formula	Unsaturation Number
369.18511	369.18545	-0.35	-0.94	$^{12}C_{26}{}^{1}H_{25}{}^{16}O_2$	14.5

Figure S9. A HR-MS spectrum of **1**$^{+}$TfO^{-}.

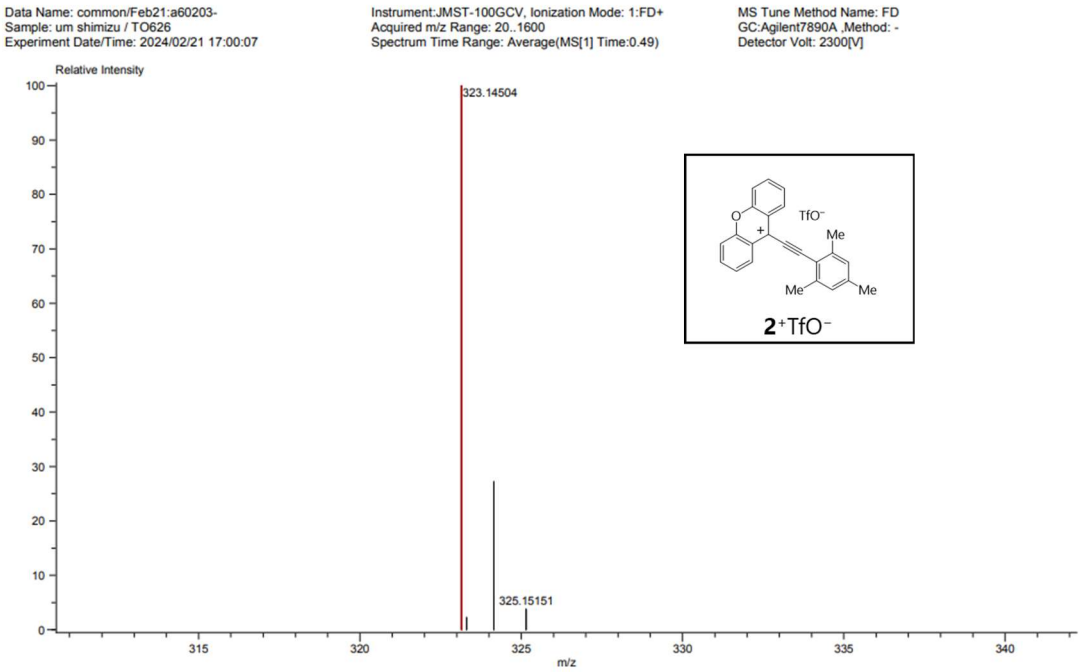

Data:a60203-
Sample Name:um shimizu / TO626
Description:
Ionization Mode:FD+
History:Determine m/z[Peak Detect[Centroid,10,Area];Correct Base[];Smooth[5];Add[Smooth[5];Average(MS[1] 0.77);,1.0];...

Acquired:2024/02/21 17:00:07
Operator:Administrator
Mass Calibration data:1600N2
Created:2024/02/21 18:23:12
Created by:Administrator

Charge number:1
Tolerance:5.00(mmu)
Unsaturation Number:-1.5 .. 20.0 (Fraction:Both)
Element:^{12}C:0 .. 100, ^{1}H:0 .. 200, ^{16}O:0 .. 10

Mass	Calc. Mass	Mass Difference (mmu)	Mass Difference (ppm)	Possible Formula	Unsaturation Number
323.14504	323.14359	1.45	4.48	$^{12}C_{24}{}^{1}H_{19}{}^{16}O_{1}$	15.5
	323.14946	-4.42	-13.69	$^{12}C_{17}{}^{1}H_{23}{}^{16}O_{6}$	6.5

Figure S10. A HR-MS spectrum of **2**$^{+}$TfO^{-}.

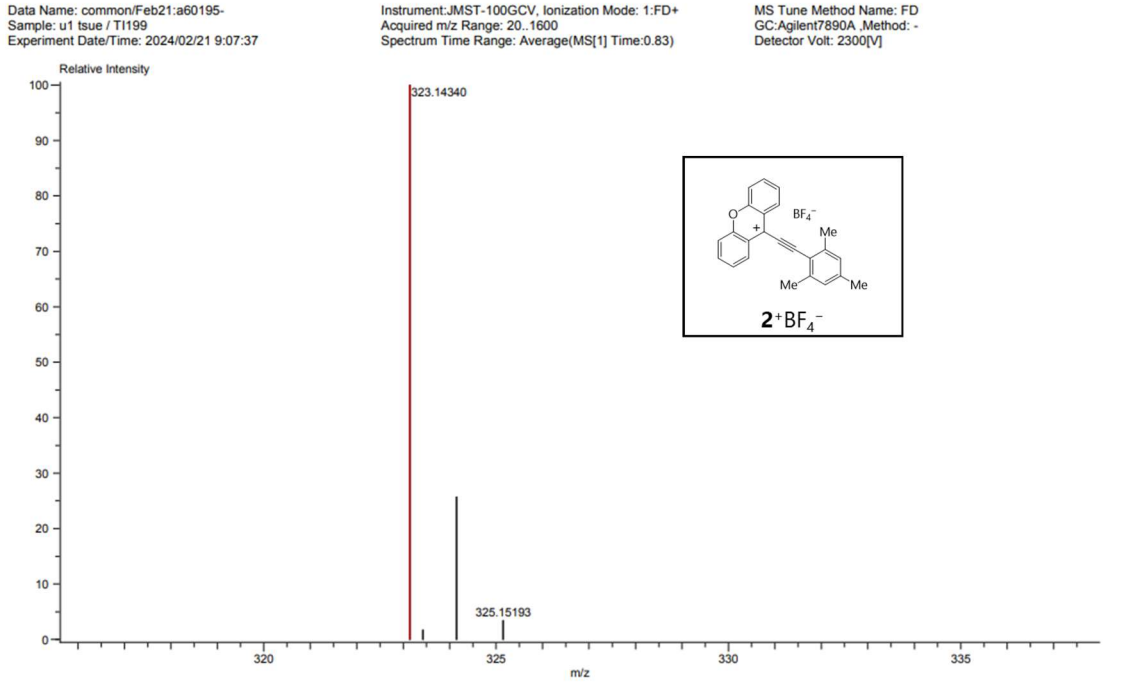

Data:a60195-
Sample Name:u1 tsue / TI199
Description:
Ionization Mode:FD+
History:Determine m/z[Peak Detect[Centroid,10,Area];Correct Base[];Smooth[5]];Add[Smooth[5];Average(MS[1] 0.51);,1.0];...

Acquired:2024/02/21 9:07:37
Operator:Administrator
Mass Calibration data:1600N2
Created:2024/02/21 9:14:38
Created by:Administrator

Charge number:1
Tolerance:5.00(mmu)
Unsaturation Number:-1.5 .. 20.0 (Fraction:Both)
Element:^{12}C:0 .. 100, ^{1}H:0 .. 200, ^{16}O:0 .. 10

Mass	Calc. Mass	Mass Difference (mmu)	Mass Difference (ppm)	Possible Formula	Unsaturation Number
323.14340	323.14359	-0.19	-0.59	$^{12}C_{24}{}^{1}H_{19}{}^{16}O_{1}$	15.5

Figure S11. A HR-MS spectrum of $\mathbf{2}^{+}BF_4^{-}$.

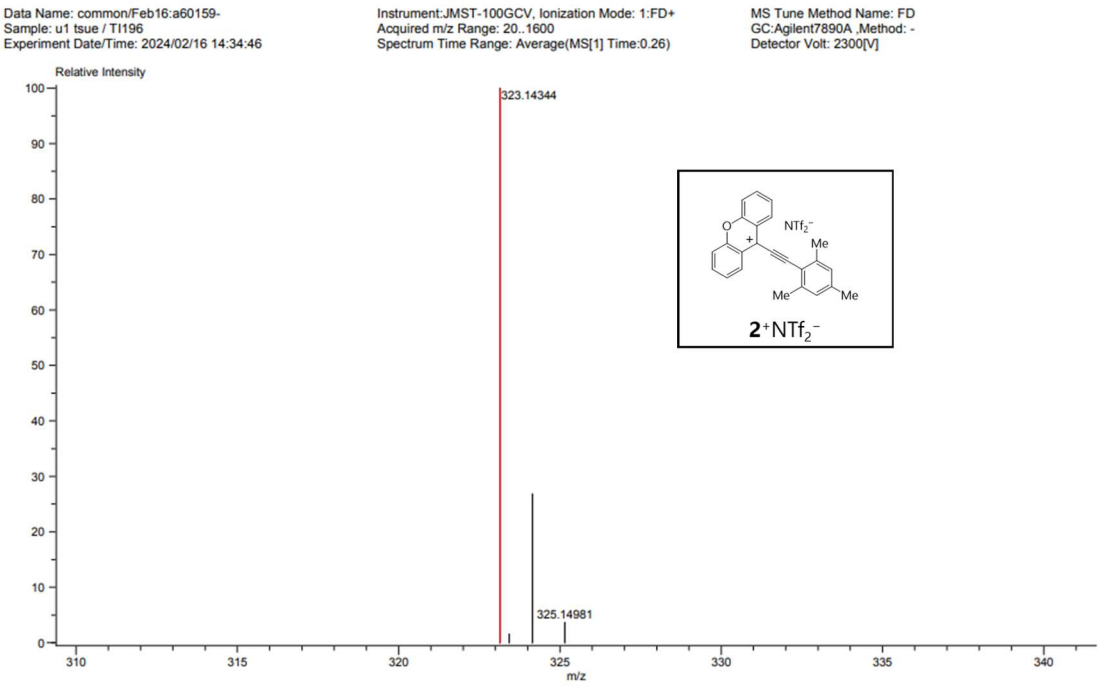

Mass	Calc. Mass	Mass Difference (mmu)	Mass Difference (ppm)	Possible Formula	Unsaturation Number
323.14344	323.14359	-0.15	-0.46	$^{12}C_{24}{}^{1}H_{19}{}^{16}O_1$	15.5

Figure S12. A HR-MS spectrum of $\mathbf{2}^{+}NTf_2^{-}$.

2.4 X-ray analyses

A suitable crystal was selected and measured on a Rigaku XtaLAB Synergy (Cu-Kα radiation, λ = 1.54184 Å) with HyPix diffractometer. Using Olex2,[3] the structure was solved with the SHELXT[4] structure solution program using Intrinsic Phasing and refined with the SHELXL[5] refinement package using Least Squares minimization.

Crystal data for **1**$^{+}$TfO^{-} (CCDC: 2346149)

Crystals, dark red needle, 0.01×0.02×0.60 mm^3, were obtained by recrystallization from CH_2Cl_2/Et_2O. Crystal Data for $C_{27}H_{25}F_3O_5S$ (*M* =518.53 g/mol): orthorhombic, space group *Pna2₁* (no. 33), *a* = 30.2694(6) Å, *b* = 7.47312(14) Å, *c* = 21.6600(5) Å, *V* = 4899.63(17) Å^3, *Z* = 8, *T* = 150 K, μ(Cu Kα) = 1.703 mm^{-1}, Dcalc = 1.406 g/cm^3, 20956 reflections measured (5.84° ≤ 2Θ ≤ 155.608°), 8411 unique (*Rint* = 0.0387, *Rsigma* = 0.0444) which were used in all calculations. The final *R1* was 0.0595 (I > 2σ(I)) and *wR2* was 0.1708 (all data).

Crystal data for **2**$^{+}$TfO^{-} (CCDC: 2346150)

Crystals, light red plate, 0.03×0.13×0.25 mm^3, were obtained by recrystallization from CH_2Cl_2/Et_2O. Crystal Data for $C_{25}H_{19}O_4F_3S$ (M =472.46 g/mol): monoclinic, space group *Cc* (no. 9), *a* = 7.3296(2) Å, *b* = 14.8403(4) Å, *c* = 19.7980(6) Å, *β* = 99.989(3)°, *V* = 2120.85(11) Å^3, *Z* = 4, *T* = 150 K, μ(Cu Kα) = 1.875 mm^{-1}, Dcalc = 1.480 g/cm^3, 16796 reflections measured (9.072° ≤ 2Θ ≤ 154.542°), 3924 unique (*Rint* = 0.0482, *Rsigma* = 0.0311) which were used in all calculations. The final *R1* was 0.0624 (I > 2σ(I)) and *wR2* was 0.1729 (all data).

Crystal data for **2**$^{+}$BF$_4^{-}$ (CCDC: 2346151)

Crystals, red plate, 0.04×0.14×0.19 mm^3, were obtained by recrystallization from CH_2Cl_2/THF.

Crystal Data for $C_{24}H_{19}BOF_4$ (M =410.20 g/mol): monoclinic, space group *P2₁/n* (no. 14), *a* = 6.8567(3) Å, *b* = 19.3806(9) Å, *c* = 14.5799(6) Å, *β* = 93.309(4)°, *V* = 1934.24(14) Å^3, *Z* = 4, *T* = 150 K, μ(Cu Kα) = 0.932 mm^{-1}, Dcalc = 1.409 g/cm^3, 16551 reflections measured (7.596° ≤ 2Θ ≤ 154.832°), 3923 unique (*Rint* = 0.0638, *Rsigma* = 0.0338) which were used in all calculations. The final *R1* was 0.0873 (I > 2σ(I)) and *wR2* was 0.2605 (all data).

Crystal data for **2**$^{+}$NTf2^{-}

Crystals were obtained by recrystallization from CH_2Cl_2/Et_2O.

Form-A (red plate, 0.06×0.16×0.25 mm^3, CCDC: 2346152)

Crystal Data for $C_{26}H_{19}NO_5F_6S_2$ (M =603.54 g/mol): triclinic, space group *P-1* (no. 2), a = 7.78770(10) Å, b = 13.5269(3) Å, c = 14.2246(3) Å, α = 115.433(2)°, β = 102.323(2)°, γ = 95.020(2)°, V = 1294.52(5) Å^3, Z = 2, T = 150 K, μ(Cu Kα) = 2.622 mm^{-1}, Dcalc = 1.548 g/cm^3, 25054 reflections measured (7.166° ≤ 2Θ ≤ 154.572°), 5270 unique (*Rint* = 0.0391, *Rsigma* = 0.0243) which were used in all calculations. The final *R1* was 0.0401 (I > 2σ(I)) and *wR2* was 0.1146 (all data).

Form-B (red block, 0.17×0.23×0.30 mm^3, CCDC: 2346153)

Crystal Data for $C_{26}H_{19}NO_5F_6S_2$ (M =603.54 g/mol): triclinic, space group *P-1* (no. 2), a = 14.24260(18) Å, b = 14.5647(2) Å, c = 15.1706(2) Å, α = 117.8081(14)°, β = 98.1608(11)°, γ = 104.9911(12)°, V = 2558.63(7) Å3, Z = 4, T = 150 K, μ(Cu Kα) = 2.653 mm^{-1}, Dcalc = 1.567 g/cm^3, 49231 reflections measured (6.752° ≤ 2Θ ≤ 154.658°), 10472 unique (*Rint* = 0.0409, *Rsigma* = 0.0268) which were used in all calculations. The final *R1* was 0.0351 (I > 2σ(I)) and *wR2* was 0.1011 (all data).

2.5 X-ray structures

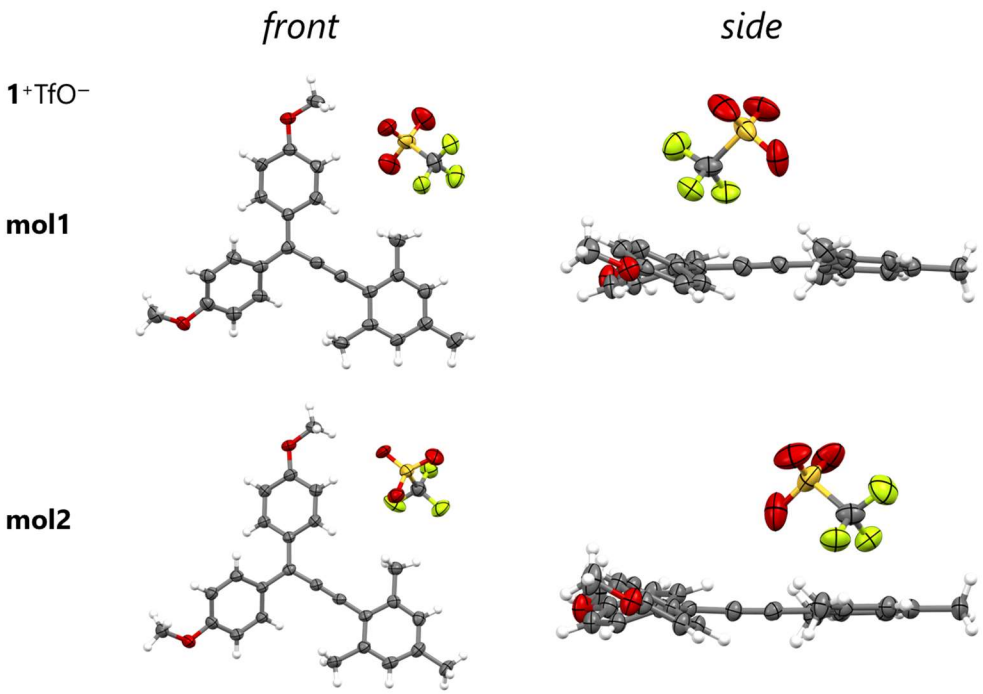

Figure S13. X-ray structures (front and side views) of **1**$^{+}$TfO^{-} at 150 K.

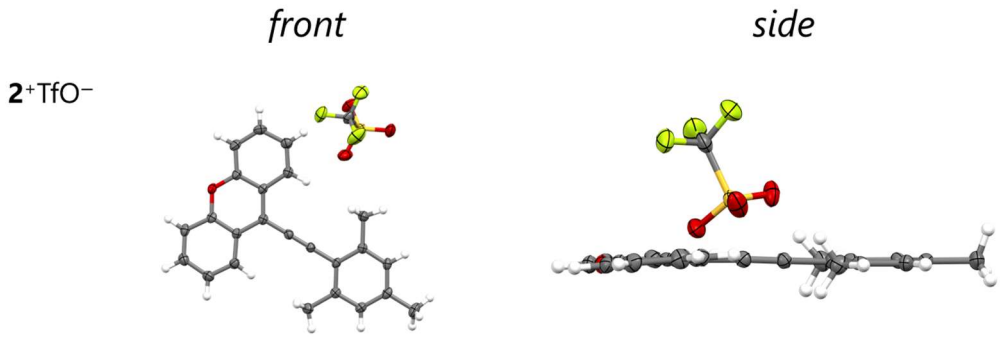

Figure S14. X-ray structures (front and side views) of **2**$^{+}$TfO^{-} at 150 K.

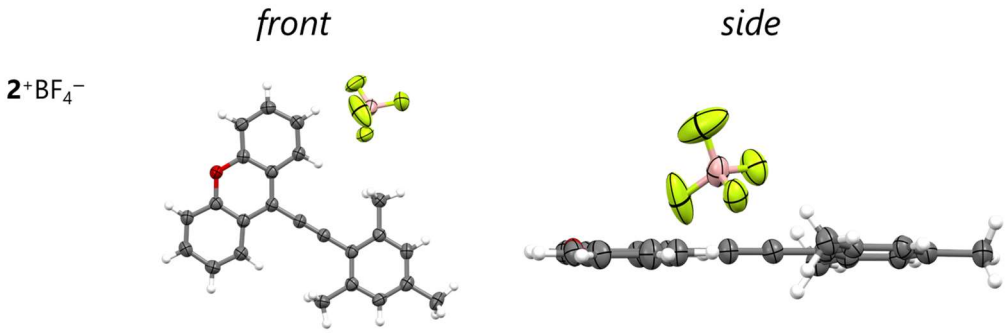

Figure S15. X-ray structures (front and side views) of **2**$^{+}$$BF_4^{-}$ at 150 K.

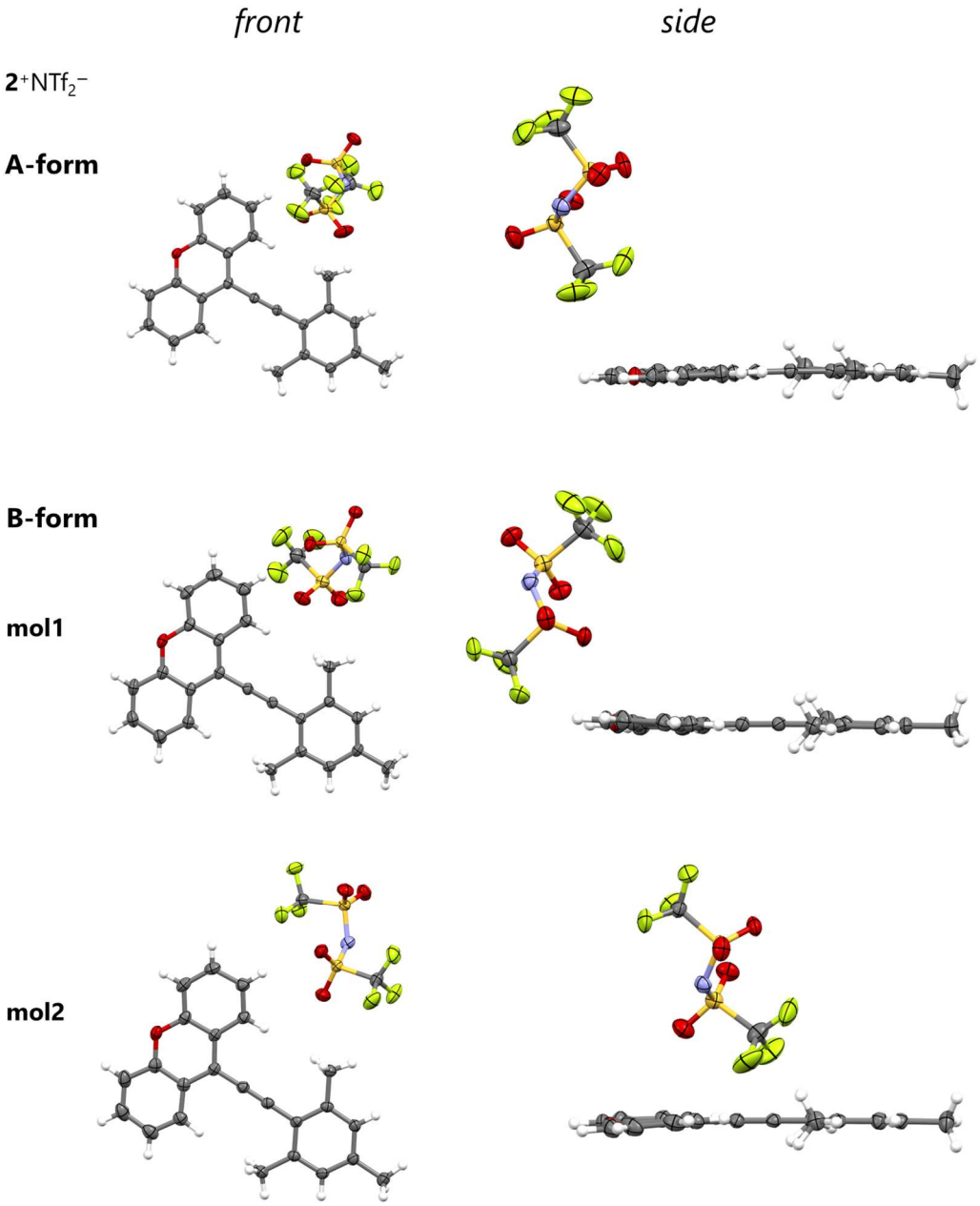

Figure S16. X-ray structures (front and side views) of $\mathbf{2}^{+}NTf_2^{-}$ at 150 K.

2.6 Crystal packings

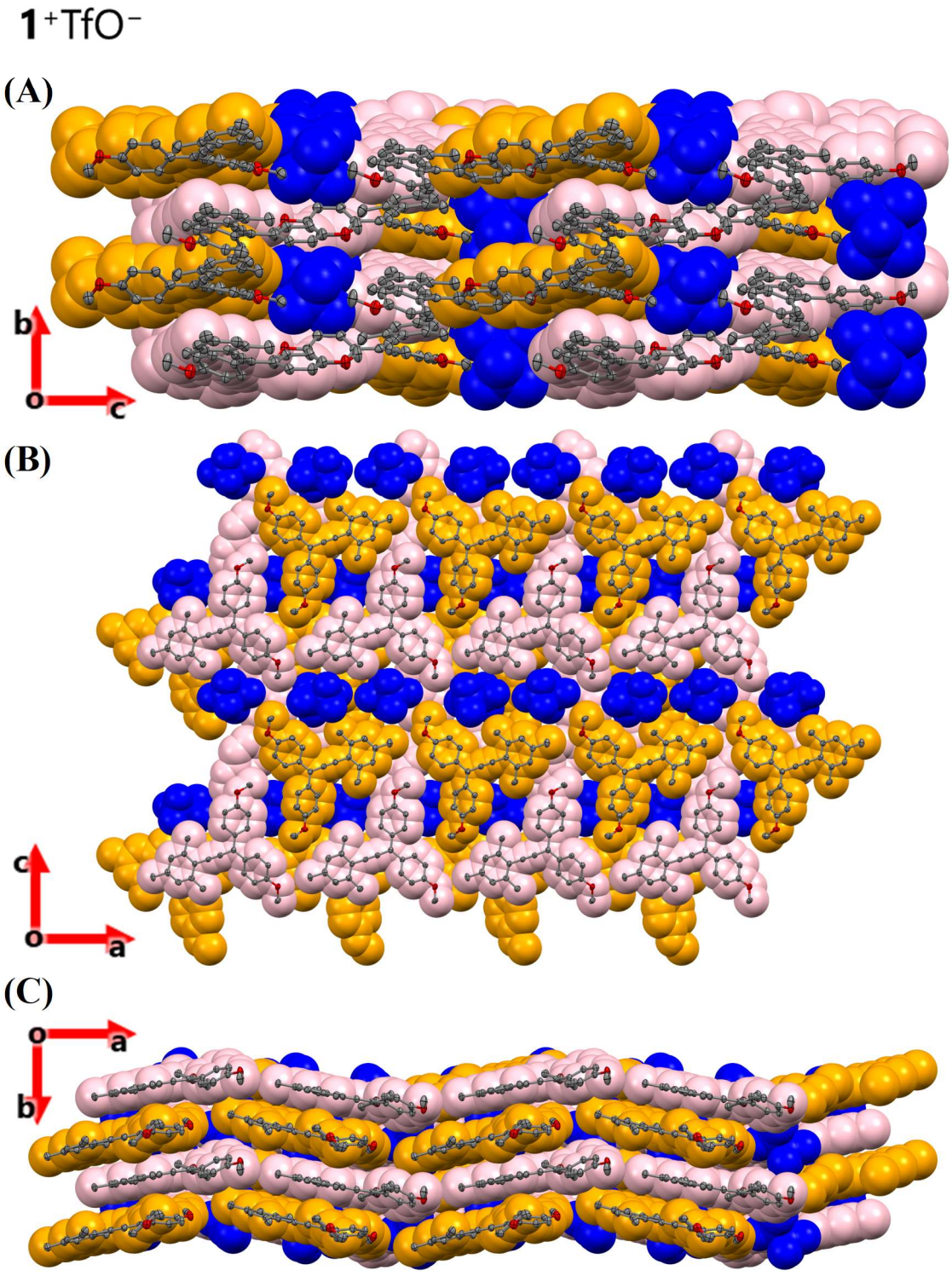

Figure S17. Crystal structures of $\mathbf{1}^{+}TfO^{-}$ at 150 K (orange: mol.1, pink: mol.2).

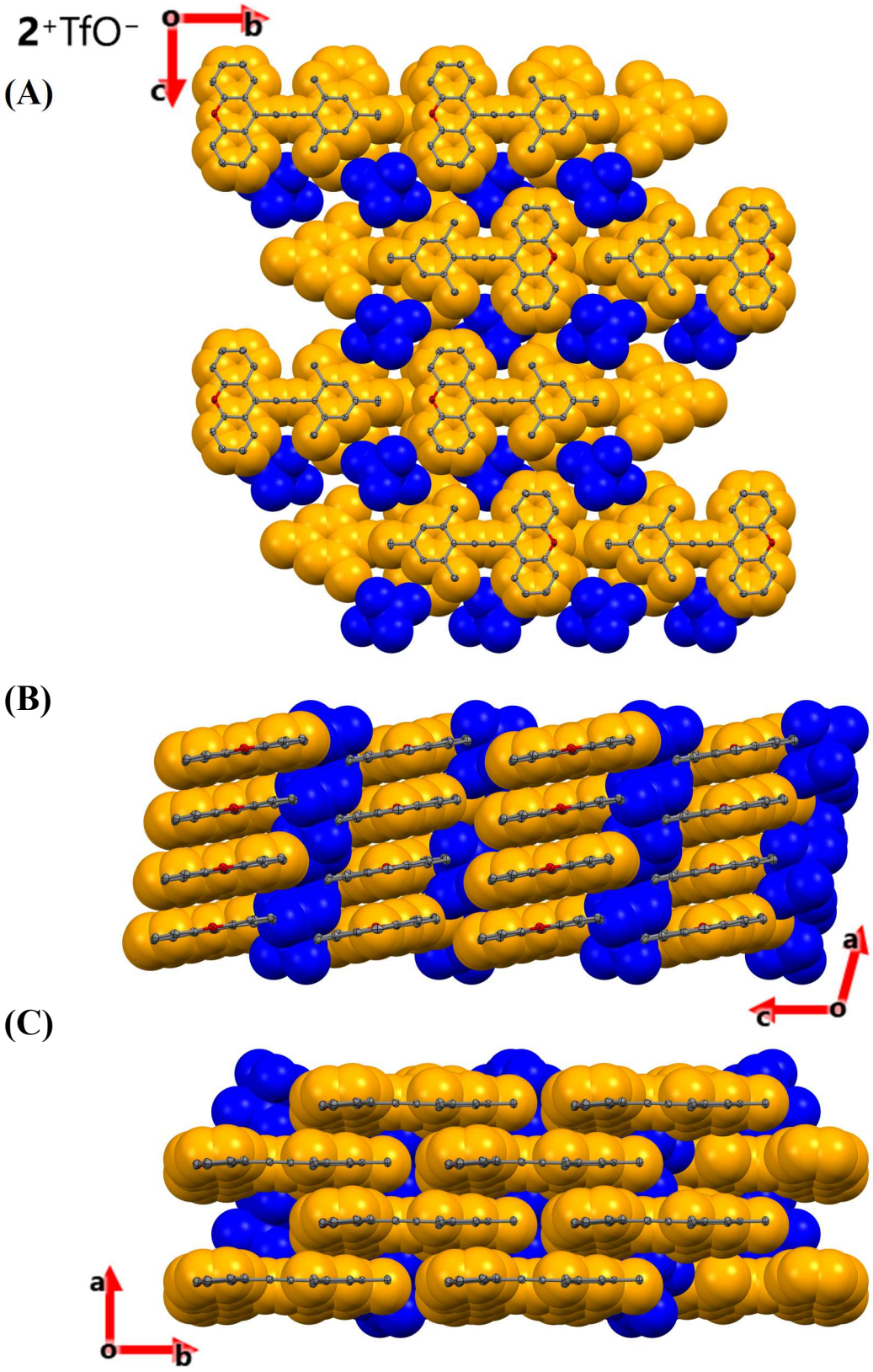

Figure S18. Crystal structures of $\mathbf{2}^{+}TfO^{-}$ at 150 K.

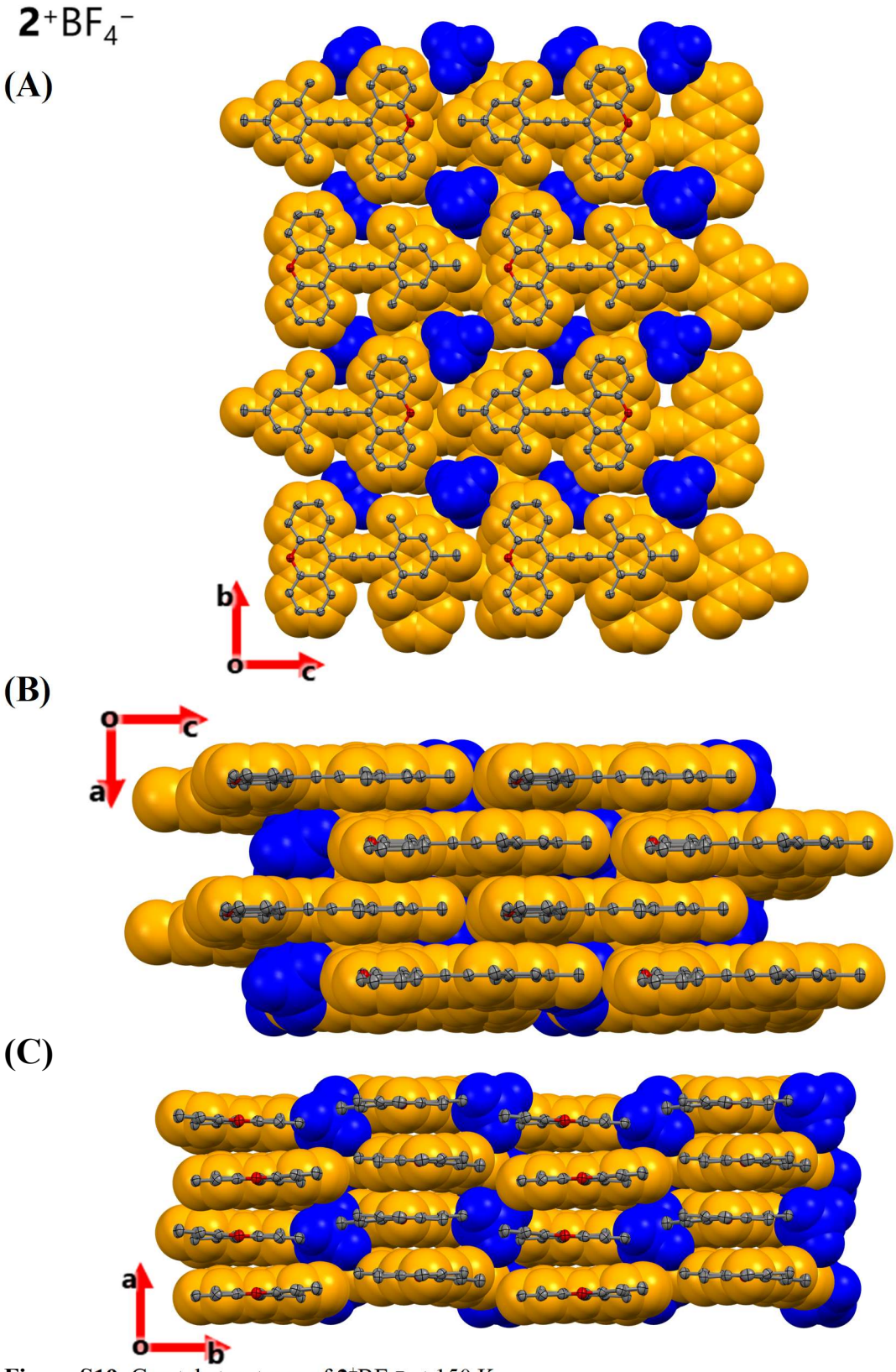

Figure S19. Crystal structures of $\mathbf{2}^{+}BF_4^{-}$ at 150 K.

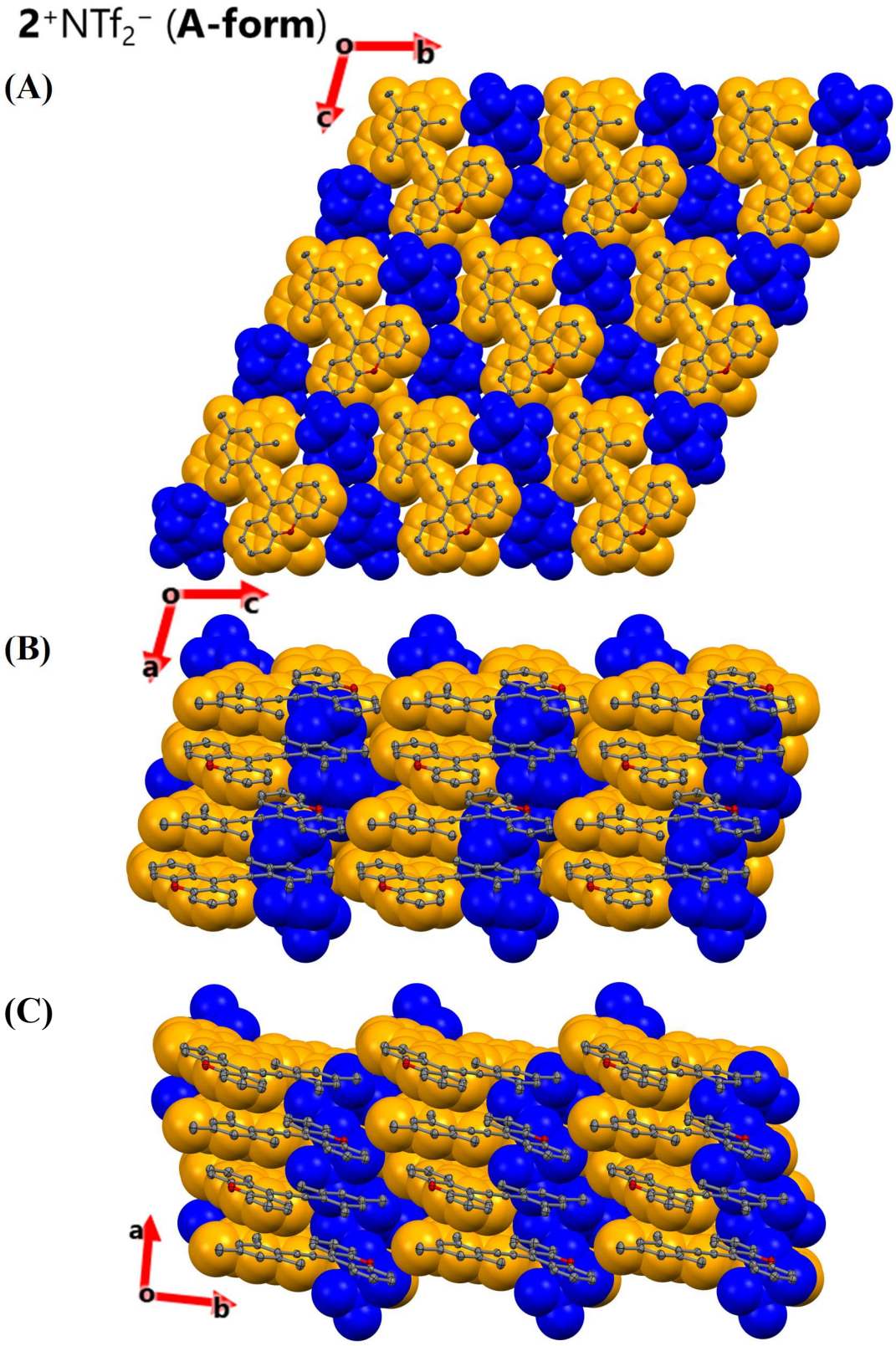

Figure S20. Crystal structures of $\mathbf{2}^{+}NTf_2^{-}$ (**A-form**) at 150 K.

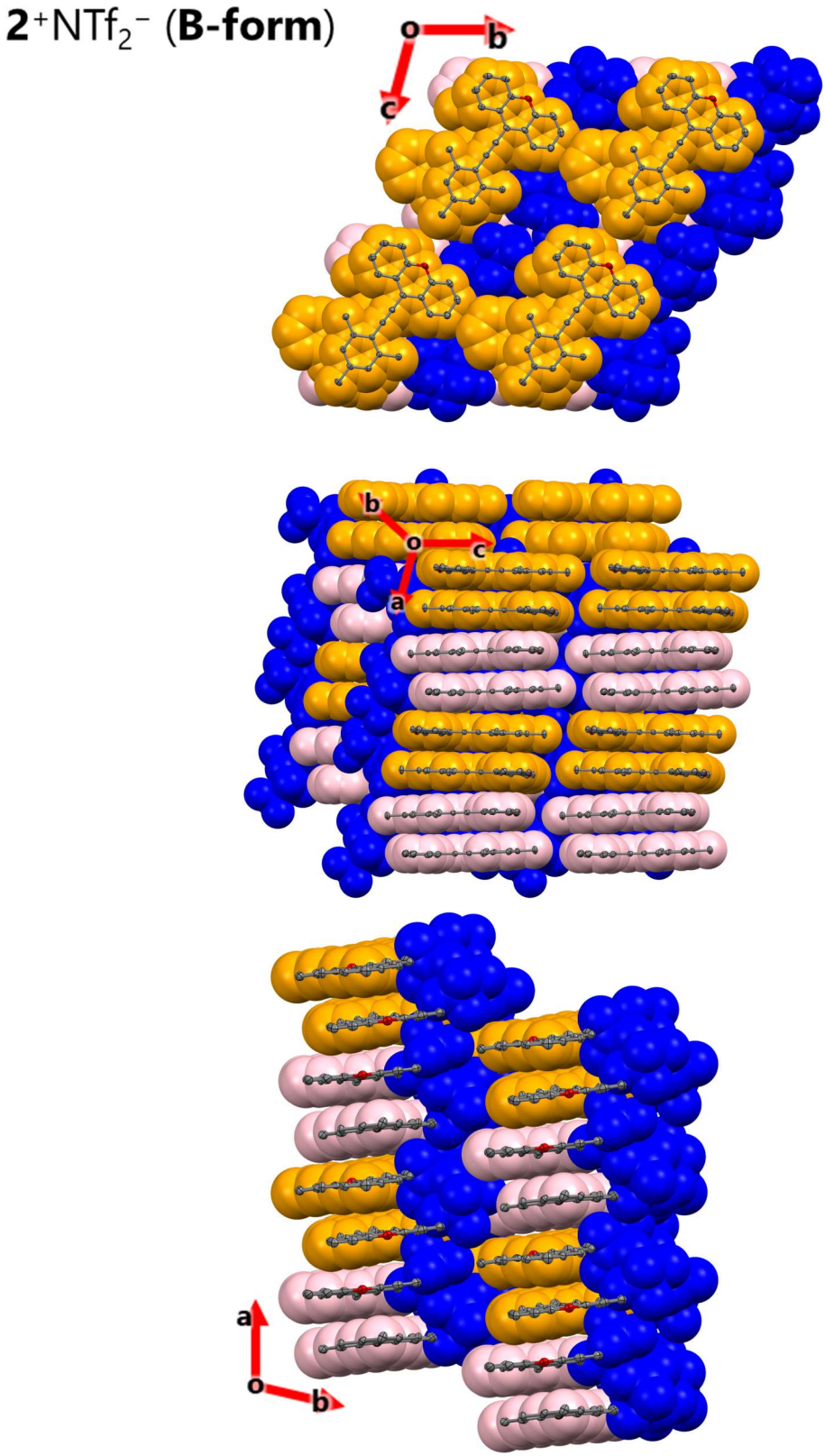

Figure S21. Crystal structures of $\mathbf{2}^{+}NTf_2^{-}$ (**B-form**) at 150 K (orange: mol.1, pink: mol.2).

.

2.7 Optical measurements

Solution

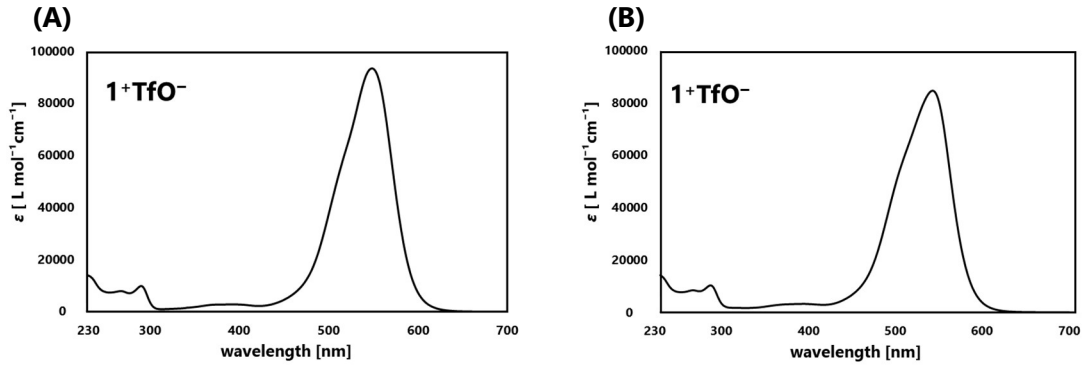

Figure S22. UV/Vis absorption spectra of **1**$^{+}$TfO^{-} (A) in CH_2Cl_2 (150 µM) and (B) in CH_3CN (150 µM).

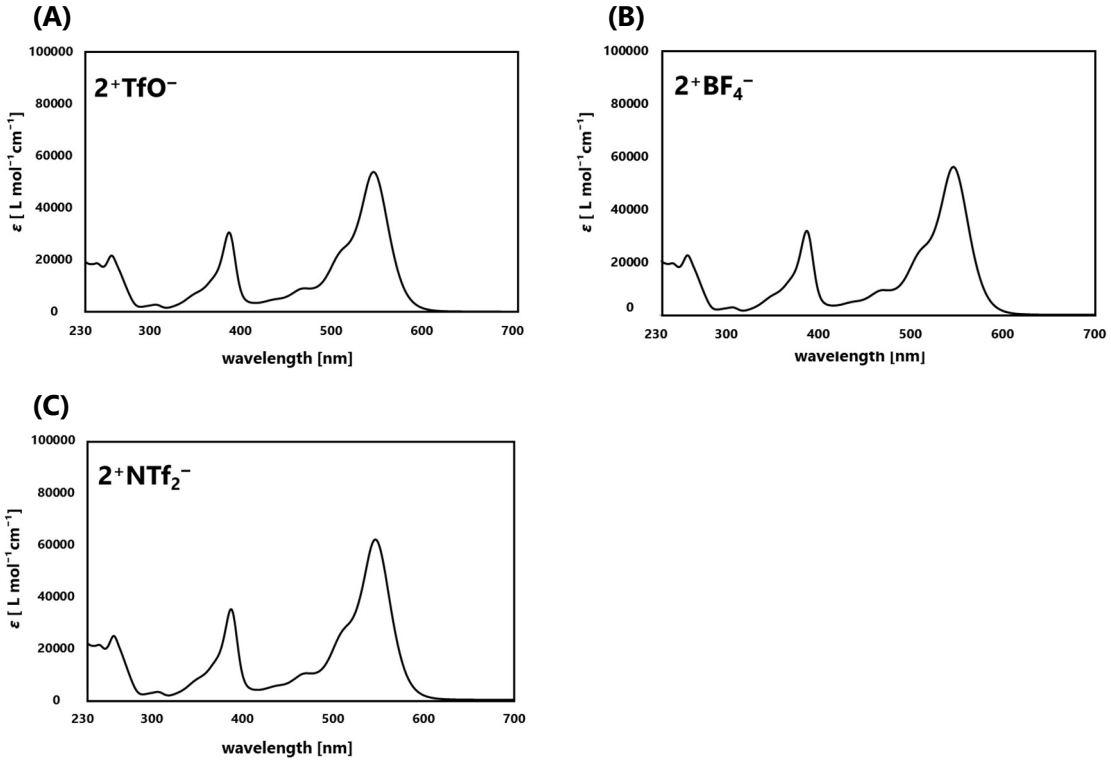

Figure S23. UV/Vis absorption spectra of (A) **2**$^{+}$TfO^{-}, (B) **2**$^{+}$$BF_4^{-}$ and (C) **2**$^{+}$$NTf_2^{-}$ in CH_2Cl_2 (25.4 µM).

3. Theoretical Studies

3.1 TD-DFT

Simulated spectra for $\mathbf{1}^+$, $\mathbf{2}^+$

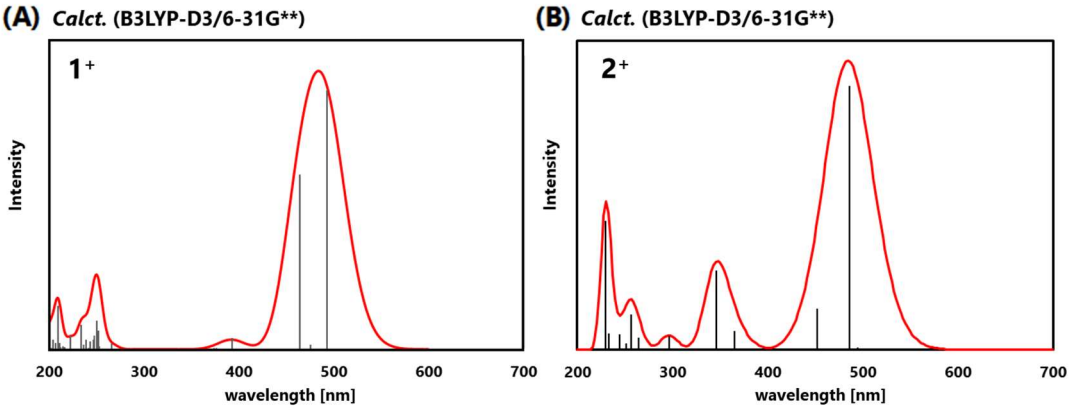

Figure S24. Simulated UV/Vis spectra by TD-DFT calculations for (A) $\mathbf{1}^+$ and (B) $\mathbf{2}^+$ at B3LYP-D3/6-31G** level of theory.

Excitation parameters for the $S_0 \rightarrow S_1$ transitions of $\mathbf{1}^+$ predicted by TD-DFT calculations at B3LYP-D3/6-31G** level

HOMO: 98, LUMO: 99

Excitation energies and oscillator strengths:

Excited State 1: Singlet-A 2.5159 eV 492.80 nm f=0.7940 <S**2>=0.000

98 -> 99 0.70515

This state for optimization and/or second-order correction.

Total Energy, E(TD-HF/TD-DFT) = -1156.00589929

Copying the excited state density for this state as the 1-particle RhoCI density.

Excited State 2: Singlet-A 2.6088 eV 475.25 nm f=0.0145 <S**2>=0.000

96 -> 99 0.67671

97 -> 99 0.20068

Excited State 3: Singlet-A 2.6713 eV 464.14 nm f=0.5350 <S**2>=0.000

96 -> 99 -0.20087

97 -> 99 0.67689

Excited State 4: Singlet-A 3.1569 eV 392.75 nm f=0.0343 <S**2>=0.000

92 -> 99 -0.33200
94 -> 99 -0.11983
95 -> 99 0.60326

Excited State 5: Singlet-A 3.2975 eV 376.00 nm f=0.0030 <S**2>=0.000
92 -> 99 -0.26262
93 -> 99 -0.32566
94 -> 99 0.56612

Excited State 6: Singlet-A 3.3160 eV 373.90 nm f=0.0027 <S**2>=0.000
92 -> 99 0.46956
93 -> 99 -0.43334
95 -> 99 0.29361

Excited State 7: Singlet-A 3.7447 eV 331.09 nm f=0.0002 <S**2>=0.000
92 -> 99 0.30320
93 -> 99 0.43339
94 -> 99 0.38273
95 -> 99 0.19837
98 ->100 0.14723

Excited State 8: Singlet-A 4.6647 eV 265.79 nm f=0.0184 <S**2>=0.000
91 -> 99 0.64544
98 ->100 0.22679

Excited State 9: Singlet-A 4.8996 eV 253.05 nm f=0.0086 <S**2>=0.000
88 -> 99 0.14177
90 -> 99 0.58912
97 ->100 -0.34128

Excited State 10: Singlet-A 4.9190 eV 252.05 nm f=0.0558 <S**2>=0.000
89 -> 99 0.56710
91 -> 99 -0.14335
98 ->100 0.31945

Excited State 11: Singlet-A 4.9384 eV 251.06 nm f=0.0535 <S**2>=0.000

88 -> 99 0.12745
89 -> 99 0.24570
90 -> 99 0.23765
97 ->100 0.48565
98 ->101 0.30660

Excited State 12: Singlet-A 4.9597 eV 249.98 nm f=0.0884 <S**2>=0.000
89 -> 99 -0.30299
90 -> 99 0.13499
91 -> 99 -0.16530
97 ->100 0.23813
97 ->101 0.15187
98 ->100 0.45386
98 ->102 -0.13272

Excited State 13: Singlet-A 5.0026 eV 247.84 nm f=0.0410 <S**2>=0.000
88 -> 99 -0.12329
96 ->100 0.16584
97 ->100 -0.21483
97 ->101 0.13816
98 ->100 0.12694
98 ->101 0.56228
98 ->104 -0.10379

Excited State 14: Singlet-A 5.0202 eV 246.97 nm f=0.0297 <S**2>=0.000
96 ->100 0.56074
98 ->101 -0.15496
98 ->104 -0.36026

Excited State 15: Singlet-A 5.0908 eV 243.55 nm f=0.0248 <S**2>=0.000
88 -> 99 0.21556
95 ->100 0.13594
97 ->101 0.53547
97 ->102 0.18023
98 ->100 -0.17371
98 ->103 -0.10472

Excited State 16: Singlet-A 5.1334 eV 241.52 nm f=0.0028 <S**2>=0.000

86 -> 99 -0.11466

87 -> 99 0.60392

88 -> 99 -0.25764

98 ->102 -0.15174

Excited State 17: Singlet-A 5.1360 eV 241.40 nm f=0.0049 <S**2>=0.000

86 -> 99 0.23305

87 -> 99 0.33938

88 -> 99 0.45393

90 -> 99 -0.13879

97 ->101 -0.10435

98 ->102 0.24308

Excited State 18: Singlet-A 5.1831 eV 239.21 nm f=0.0280 <S**2>=0.000

86 -> 99 -0.29451

97 ->101 0.21918

98 ->102 0.52235

98 ->103 0.19032

Excited State 19: Singlet-A 5.2084 eV 238.05 nm f=0.0017 <S**2>=0.000

86 -> 99 0.57374

88 -> 99 -0.25374

97 ->101 0.13298

98 ->102 0.10370

98 ->103 0.22739

Excited State 20: Singlet-A 5.2582 eV 235.79 nm f=0.0151 <S**2>=0.000

97 ->102 0.42821

97 ->103 0.37482

98 ->101 0.15406

98 ->103 0.31074

Excited State 21: Singlet-A 5.3141 eV 233.31 nm f=0.0745 <S**2>=0.000

88 -> 99 0.17910

90 -> 99 -0.10916
97 ->100 -0.10891
97 ->102 -0.22960
97 ->103 -0.16789
98 ->102 -0.28033
98 ->103 0.50459

Excited State 22: Singlet-A 5.4254 eV 228.52 nm f=0.0023 <S**2>=0.000
85 -> 99 0.66972
97 ->103 -0.10812

Excited State 23: Singlet-A 5.5687 eV 222.65 nm f=0.0408 <S**2>=0.000
93 ->101 0.10671
94 ->101 -0.10752
95 ->102 -0.10780
97 ->101 0.14919
97 ->102 -0.39217
97 ->103 0.46923
98 ->100 -0.12147

Excited State 24: Singlet-A 5.6378 eV 219.92 nm f=0.0004 <S**2>=0.000
96 ->101 0.70300

Excited State 25: Singlet-A 5.7435 eV 215.87 nm f=0.0069 <S**2>=0.000
81 -> 99 -0.16110
83 -> 99 0.50341
84 -> 99 -0.34851
98 ->105 0.19714

Excited State 26: Singlet-A 5.7627 eV 215.15 nm f=0.0007 <S**2>=0.000
83 -> 99 0.28855
84 -> 99 0.56815
98 ->105 0.21499

Excited State 27: Singlet-A 5.7792 eV 214.54 nm f=0.0081 <S**2>=0.000
96 ->100 -0.15630

96 ->102 0.65352
98 ->104 -0.16896

Excited State 28: Singlet-A 5.7928 eV 214.03 nm f=0.0003 <S**2>=0.000
83 -> 99 -0.18705
84 -> 99 -0.17676
92 ->100 -0.28011
93 ->100 0.14488
94 ->100 0.14396
95 ->100 0.31564
98 ->105 0.40963
98 ->106 0.14617

Excited State 29: Singlet-A 5.8025 eV 213.67 nm f=0.0023 <S**2>=0.000
83 -> 99 -0.21098
92 ->100 0.37273
93 ->100 -0.14199
95 ->100 -0.24623
96 ->104 -0.10608
98 ->105 0.36091
98 ->106 0.18216

Excited State 30: Singlet-A 5.8547 eV 211.77 nm f=0.0069 <S**2>=0.000
82 -> 99 0.67983

Excited State 31: Singlet-A 5.8821 eV 210.78 nm f=0.0185 <S**2>=0.000
96 ->100 -0.14044
96 ->102 -0.17582
96 ->103 0.63509
98 ->104 -0.19599

Excited State 32: Singlet-A 5.9333 eV 208.96 nm f=0.1336 <S**2>=0.000
96 ->100 0.30181
96 ->102 0.17140
96 ->103 0.28488
96 ->105 0.18482

98 ->104 0.49462

Excited State 33: Singlet-A 5.9485 eV 208.43 nm f=0.0009 <S**2>=0.000
97 ->104 0.70234

Excited State 34: Singlet-A 6.0014 eV 206.59 nm f=0.0188 <S**2>=0.000
94 ->100 0.61092
95 ->100 -0.26400

Excited State 35: Singlet-A 6.0789 eV 203.96 nm f=0.0297 <S**2>=0.000
92 ->100 0.32412
93 ->100 -0.33845
94 ->100 0.20743
95 ->100 0.42298
95 ->102 0.10918

Excited State 36: Singlet-A 6.1325 eV 202.18 nm f=0.0049 <S**2>=0.000
81 -> 99 -0.37952
83 -> 99 -0.12078
92 ->100 0.27251
93 ->100 0.39812
94 ->101 -0.13107
95 ->100 0.12927
95 ->101 -0.14959
96 ->104 0.10725

Excited State 37: Singlet-A 6.1471 eV 201.70 nm f=0.0022 <S**2>=0.000
81 -> 99 0.49362
83 -> 99 0.16006
92 ->100 0.12365
93 ->100 0.22189
94 ->101 -0.25785
95 ->101 -0.23271
97 ->105 0.10402

Excited State 38: Singlet-A 6.1773 eV 200.71 nm f=0.0418 <S**2>=0.000

81 -> 99 0.14902
92 ->100 0.21202
93 ->100 0.25395
93 ->101 0.13869
94 ->101 0.14918
95 ->101 0.42943
95 ->102 -0.17382
97 ->105 -0.22546

Excited State 39: Singlet-A 6.2389 eV 198.73 nm f=0.0030 <S**2>=0.000
79 -> 99 -0.10248
94 ->101 0.31332
95 ->102 -0.11017
97 ->105 0.58363
97 ->106 0.10584

Excited State 40: Singlet-A 6.2758 eV 197.56 nm f=0.0367 <S**2>=0.000
76 -> 99 0.10418
78 -> 99 0.23735
79 -> 99 0.53451
83 -> 99 0.10592
94 ->101 -0.16538
95 ->101 0.16398
97 ->105 0.18221

Excitation parameters for the $S_0 \rightarrow S_1$ transitions of $\mathbf{2}^+$ predicted by TD-DFT calculations at B3LYP-D3/6-31G** level

HOMO:85, LUMO:86

Excitation energies and oscillator strengths:

Excited State 1: Singlet-A 2.5054 eV 494.87 nm f=0.0061 <S**2>=0.000

84 -> 86 0.70611

This state for optimization and/or second-order correction.

Total Energy, E(TD-HF/TD-DFT) = -1000.96655168

Copying the excited state density for this state as the 1-particle RhoCI density.

Excited State 2: Singlet-A 2.5498 eV 486.24 nm f=0.6835 <S**2>=0.000

83 -> 86 0.18118

85 -> 86 0.68438

Excited State 3: Singlet-A 2.7441 eV 451.83 nm f=0.1058 <S**2>=0.000

83 -> 86 0.67880

85 -> 86 -0.18463

Excited State 4: Singlet-A 3.3344 eV 371.83 nm f=0.0000 <S**2>=0.000

80 -> 86 0.70308

Excited State 5: Singlet-A 3.3970 eV 364.98 nm f=0.0489 <S**2>=0.000

81 -> 86 0.59972

82 -> 86 0.36405

Excited State 6: Singlet-A 3.5850 eV 345.84 nm f=0.2053 <S**2>=0.000

81 -> 86 -0.36800

82 -> 86 0.58593

83 -> 88 0.13353

Excited State 7: Singlet-A 4.1842 eV 296.32 nm f=0.0361 <S**2>=0.000

79 -> 86 0.65386

85 -> 87 -0.24430

Excited State 8: Singlet-A 4.6789 eV 264.99 nm f=0.0312 <S**2>=0.000

85 -> 88 0.69987

Excited State 9: Singlet-A 4.8286 eV 256.77 nm f=0.0917 <S**2>=0.000
78 -> 86 -0.14603
79 -> 86 0.19699
82 -> 88 0.10222
83 -> 87 0.12388
84 -> 91 -0.10396
85 -> 87 0.60888
85 -> 90 -0.12797

Excited State 10: Singlet-A 4.9210 eV 251.95 nm f=0.0174 <S**2>=0.000
84 -> 87 0.62769
85 -> 91 0.29306

Excited State 11: Singlet-A 5.0272 eV 246.63 nm f=0.0000 <S**2>=0.000
77 -> 86 0.69615

Excited State 12: Singlet-A 5.0652 eV 244.78 nm f=0.0007 <S**2>=0.000
76 -> 86 0.69196

Excited State 13: Singlet-A 5.0715 eV 244.47 nm f=0.0403 <S**2>=0.000
83 -> 88 -0.38149
85 -> 89 0.56260

Excited State 14: Singlet-A 5.0792 eV 244.10 nm f=0.0000 <S**2>=0.000
78 -> 86 0.66047
81 -> 88 0.10608
82 -> 88 0.13342

Excited State 15: Singlet-A 5.1849 eV 239.13 nm f=0.0001 <S**2>=0.000
84 -> 88 0.70592

Excited State 16: Singlet-A 5.2124 eV 237.86 nm f=0.0002 <S**2>=0.000
74 -> 86 0.69618

Excited State 17: Singlet-A 5.3170 eV 233.18 nm f=0.0419 <S**2>=0.000

75 -> 86 0.16395

83 -> 87 0.65420

85 -> 87 -0.11121

Excited State 18: Singlet-A 5.3888 eV 230.08 nm f=0.3330 <S**2>=0.000

82 -> 86 -0.10614

82 -> 87 -0.24638

83 -> 88 0.49257

85 -> 89 0.40899

Excited State 19: Singlet-A 5.4830 eV 226.12 nm f=0.0000 <S**2>=0.000

75 -> 86 0.58709

83 -> 87 -0.14899

85 -> 90 -0.33161

Excited State 20: Singlet-A 5.5923 eV 221.70 nm f=0.0000 <S**2>=0.000

72 -> 86 0.23405

73 -> 86 -0.36600

85 -> 92 0.53666

3.2 Optimized structures

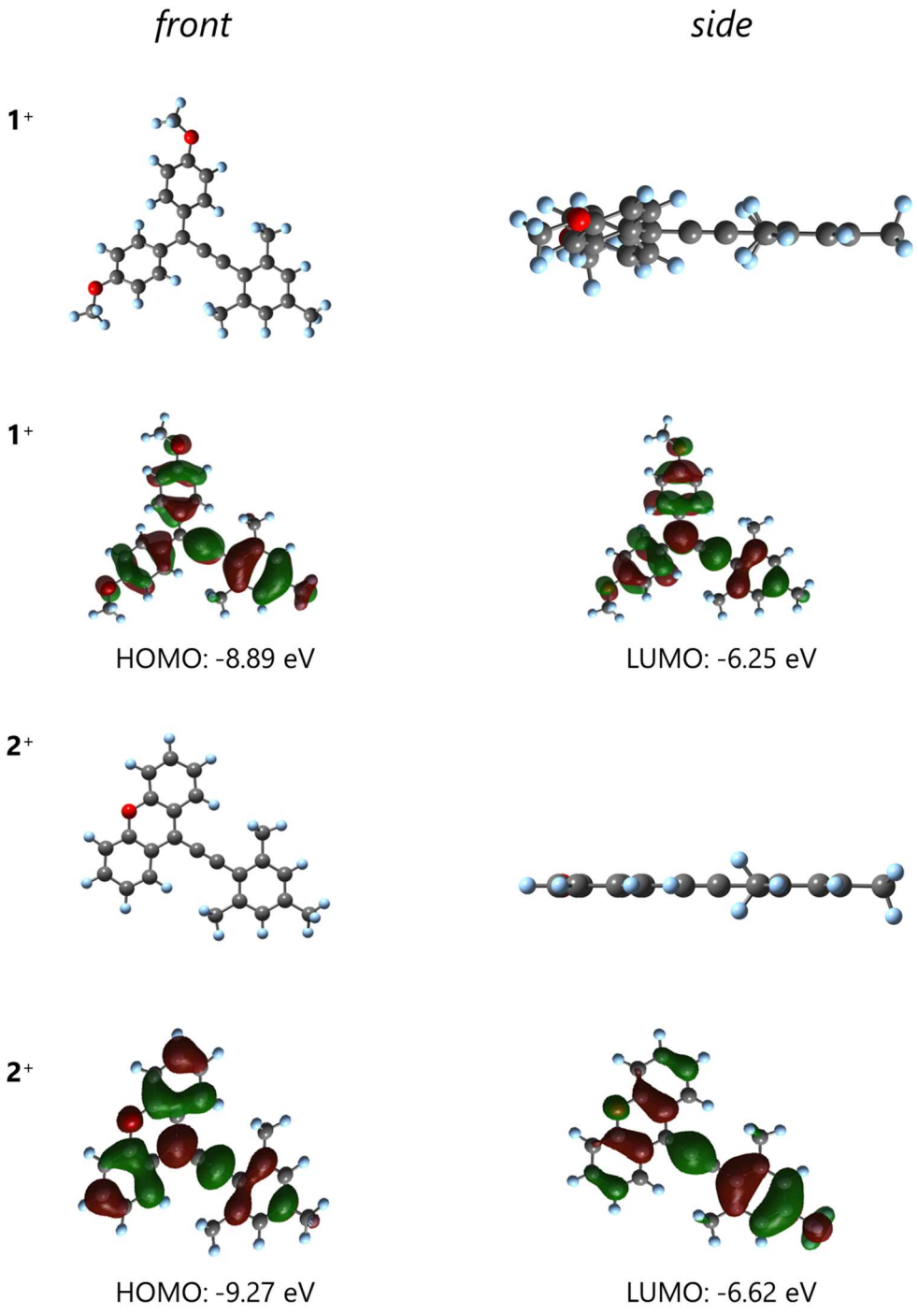

Figure S25. Optimized structures and Kohn–Sham orbitals for propargyl cations $\mathbf{1}^+$ and $\mathbf{2}^+$ calculated at the B3LYP-D3/6-31G** level.

3.3 Cartesian coordinates of optimized structures of ***1***$^{+}$

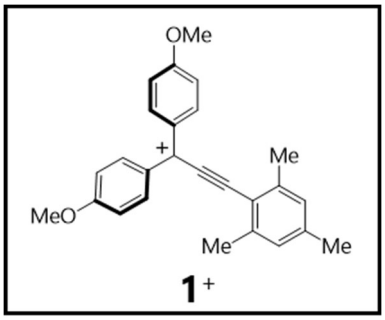

center number	Symbol	x	y	z
1	C	0.901240857	0.029235187	-0.057760688
2	C	-0.483431143	-0.068946507	-0.034128352
3	C	-1.708535253	-0.160361153	-0.016541801
4	C	-3.103370904	-0.264371998	0.003060069
5	C	-3.898883613	0.917880487	-0.084349994
6	C	-3.712443493	-1.550879841	0.113183520
7	C	-5.280166627	0.783876540	-0.059043526
8	C	-5.098785172	-1.621638935	0.133270801
9	C	-5.900333364	-0.471931834	0.046125301
10	H	-5.899316392	1.674286478	-0.121737080
11	H	-5.577348708	-2.592999244	0.219823464
12	C	1.674669777	-1.195067446	-0.077598700
13	C	2.980197893	-1.258812470	0.467609826
14	C	1.110215149	-2.396357957	-0.586897125
15	C	3.699371593	-2.441824195	0.488460561
16	H	3.409746666	-0.377831355	0.930231309
17	C	1.822120435	-3.572475677	-0.588646029
18	H	0.111715113	-2.371954282	-1.008932444
19	C	3.130155100	-3.612214084	-0.052445791
20	H	4.683199169	-2.459618907	0.939435855
21	H	1.409581996	-4.486899244	-0.999662026
22	C	1.497202312	1.350002442	-0.063645988
23	C	2.762142333	1.598388855	-0.662605133
24	C	0.797367062	2.453598494	0.481339506
25	C	3.297721817	2.866968917	-0.690648611
26	H	3.290128568	0.789716556	-1.154174438
27	C	1.333676462	3.727786411	0.476092661
28	H	-0.169611645	2.286300144	0.943258028
29	C	2.597877094	3.947848315	-0.111490584

30	H	4.248630764	3.070032838	-1.169961732
31	H	0.782215813	4.542461188	0.927682982
32	O	3.732662440	-4.805301448	-0.096371117
33	O	3.210789166	5.134925491	-0.181331032
34	C	5.065999133	-4.948492224	0.412653324
35	H	5.101897597	-4.724897527	1.484200163
36	H	5.330057511	-5.991954425	0.247656124
37	H	5.763606664	-4.301349989	-0.129445236
38	C	2.570022162	6.300094655	0.355448252
39	H	2.404237391	6.194953856	1.432970582
40	H	3.259151473	7.122640839	0.170124542
41	H	1.619790413	6.494219836	-0.153328317
42	C	-2.868222892	-2.795698674	0.188458202
43	H	-2.354382819	-2.972929400	-0.763920906
44	H	-2.096719860	-2.711159968	0.959865886
45	H	-3.479333803	-3.673832742	0.405879408
46	C	-3.249202264	2.273206309	-0.180705361
47	H	-2.722769280	2.517971626	0.749590305
48	H	-2.510097315	2.305695501	-0.987152344
49	H	-3.991010800	3.053790907	-0.360505570
50	C	-7.400229178	-0.585606245	0.035101010
51	H	-7.874599064	0.302596903	0.460558253
52	H	-7.762866621	-0.687567525	-0.995568739
53	H	-7.741767425	-1.463908655	0.588957027

3.4 Cartesian coordinates of optimized structures of $\mathbf{2}^{+}$

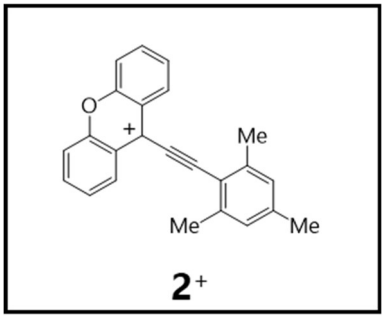

center number	Symbol	x	y	z
1	C	4.737797233	-1.210131582	-0.008864216
2	C	5.450892014	0.000272816	-0.008401716
3	C	4.737819882	1.210565857	-0.008857053
4	C	3.350558874	1.242553129	-0.00475919
5	C	2.646284689	0.000197291	-0.002615769
6	C	3.350636298	-1.242190060	-0.004747603
7	C	1.247936322	0.000165165	-0.001935787
8	C	0.020052344	0.000131923	-0.000939735
9	C	-1.366003254	0.000025031	0.000054949
10	C	-2.103925841	1.231886662	0.000609316
11	C	-1.487729616	2.509160767	-0.000104594
12	C	-3.519668217	1.178888751	0.001842337
13	C	-2.252836356	3.655067249	0.000370714
14	H	-0.405156538	2.562147507	-0.001161137
15	C	-4.299776401	2.339075049	0.00233269
16	C	-3.662947344	3.568272427	0.001593312
17	H	-1.774525222	4.628250647	-0.000229485
18	H	-5.379592206	2.246712585	0.003261064
19	C	-2.103735168	-1.231948973	0.00051176
20	C	-3.519488698	-1.179154885	0.001877575
21	C	-1.487343952	-2.509134133	-0.000292091
22	C	-4.299417661	-2.339472186	0.002534147
23	C	-2.252274497	-3.655150663	0.000299085
24	H	-0.404764404	-2.561949176	-0.001491451
25	C	-3.662407710	-3.568564814	0.001752496
26	H	-5.379248929	-2.247275502	0.003614286
27	H	-1.773828148	-4.628267555	-0.000404147
28	O	-4.188241326	-0.000194408	0.002595675
29	H	-4.257186157	4.476099022	0.001919023

30	H	-4.256510155	-4.476480903	0.002251374
31	C	2.602226899	2.549527815	-0.005741683
32	H	1.959625534	2.633182170	-0.889366993
33	H	1.960124813	2.634528688	0.878100995
34	H	3.289289520	3.397672355	-0.006536492
35	C	2.602303149	-2.549167498	-0.005822356
36	H	1.960324562	-2.634308328	0.878090263
37	H	1.959584909	-2.632704794	-0.889376656
38	H	3.289374077	-3.397305614	-0.00686525
39	H	5.288329023	2.146870538	-0.013563212
40	H	5.288391211	-2.146408767	-0.013611568
41	C	6.954183664	-0.000277382	0.022390508
42	H	7.367617413	0.893423555	-0.451908881
43	H	7.308493709	-0.013206909	1.060966157
44	H	7.366767713	-0.883010780	-0.472975866

4. References

[1] J. M. Frisch, W. G. Trucks, B. H. Schlegel, E. G. Scuseria, A. M. Robb, R. J. Cheeseman, G. Scalmani, V. Barone, A. G. Petersson, H. Nakatsuji, X. Li, M. Caricato, V. A. Marenich, J. Bloino, G. B. Janesko, R. Gomperts, B. Mennucci, P. H. Hratchian, V. J. Ortiz, F. A. Izmaylov, L. J. Sonnenberg, D. Williams-Young, F. Ding, F. Lipparini, F. Egidi, J. Goings, B. Peng, A. Petrone, T. Henderson, D. Ranasinghe, G. V. Zakrzewski, J. Gao, N. Rega, G. Zheng, W. Liang, M. Hada, M. Ehara, K. Toyota, R. Fukuda, J. Hasegawa, M. Ishida, T. Nakajima, Y. Honda, O. Kitao, H. Nakai, T. Vreven, K. Throssell, A. J. Montgomery, Jr., E. J. Peralta, F. Ogliaro, J. M. Bearpark, J. J. Heyd, N. E. Brothers, N. K. Kudin, N. V. Staroverov, A. T. Keith, R. Kobayashi, J. Normand, K. Raghavachari, P. A. Rendell, C. J. Burant, S. S. Iyengar, J. Tomasi, M. Cossi, M. J. Millam, M. Klene, C. Adamo, R. Cammi, W. J. Ochterski, L. R. Martin, K. Morokuma, O. Farkas, B. J. Foresman, J. D. Fox, **2019**, Gaussian, Inc., Wallingford CT.

[2] C. M. Le, P. J. C. Menzies, D. A. Petrone, M. Lautens, *Angew. Chem. Int. Ed.* **2015**, *54*, 254-257.

[3] O. V. Dolomanov, L. J. Bourhis, R. J. Gildea, J. A. K. Howard, H. Puschmann, *J. Appl. Crystallogr.* **2009**, *42*, 339–341.

[4] G. M. Sheldrick, *Acta Crystallogr. Sect. A Found. Adv.* **2015**, *71*, 3–8.

[5] G. M. Sheldrick, *Acta Crystallogr. Sect. C Struct. Chem.* **2015**, *71*, 3–8